Distinct gene expression and secondary metabolite profiles in *Suppressed systemin-mediated signaling2* (*spr2*) tomato mutants having impaired mycorrhizal colonization

Kena Casarrubias-Castillo [1] , Josaphat M Montero-Vargas [2] , Nicole Dabdoub-González [3] , Robert Winkler [4] , Norma A Martinez-Gallardo [4] , Julia Zañudo-Hernández [1] , Hamlet Aviles-Arnaut [Corresp., 3] , John P Délano-Frier [Corresp. 4]

[1] Centro Universitario de Ciencias Biológicas y Agropecuarias, Universidad de Guadalajara, Zapopan, Jalisco, Mexico

[2] Departamento de Investigación en Inmunogenética y Alergia, Instituto Nacional de Enfermedades Respiratorias "Ismael Cosío Villegas", Mexico City, Mexico

[3] Instituto de Biotecnología de la Facultad de Ciencias Biológicas, Universidad Autónoma de Nuevo León, Nicolas de los Garza, Nuevo Leon, Mexico

[4] Departamento de Biotecnología y Bioquímica, Centro de Investigación y de Estudios Avanzados del IPN-Unidad Irapuato, Irapuato, Guanajuato, México

Corresponding Authors: Hamlet Aviles-Arnaut, John P Délano-Frier
Email address: hamlet.avilesarn@uanl.edu.mx, john.delano@cinvestav.mx

Arbuscular mycorrhizal fungi (AMF) colonization, sampled at 32 to 50 days post-inoculation (dpi), was significantly reduced in *Suppressor of prosystemin-mediated responses2* (*spr2*) mutant tomato plants impaired in the *ω-3 FATTY ACID DESATURASE7* (*FAD7*) gene that limits the generation of linolenic acid and, consequently, the wound-responsive jasmonic acid (JA) burst. Contrary to wild-type (WT) plants, JA levels in root and leaves of *spr2* mutants remained unchanged in response to AMF colonization, further supporting its regulatory role in the AM symbiosis. Decreased AMF colonization in *spr2* plants was also linked to alterations associated with a disrupted FAD7 function, such as enhanced salicylic acid (SA) levels and SA-related defense gene expression and a reduction in fatty acid content in both mycorrhizal *spr2* roots and leaves. Transcriptomic data revealed that lower mycorrhizal colonization efficiency in *spr2* mutants coincided with the modified expression of key genes controlling gibberellin and ethylene signaling, brassinosteroid, ethylene, apocarotenoid and phenylpropanoid synthesis, and the wound response. Targeted metabolomic analysis, performed at 45 dpi, revealed augmented contents of L-threonic acid and DL-malic acid in colonized *spr2* roots which suggested unfavorable conditions for AMF colonization. Additionally, time- and genotype-dependent changes in root steroid glycoalkaloid levels, including tomatine, suggested that these metabolites might positively regulate the AM symbiosis in tomato. Untargeted metabolomic analysis demonstrated that the tomato root metabolomes were distinctly affected by genotype, mycorrhizal colonization and colonization time. In conclusion, reduced AMF colonization efficiency in *spr2* mutants is probably caused by multiple and interconnected JA-dependent and independent gene expression and metabolomic alterations.

1 **Distinct gene expression and secondary metabolite profiles in S*uppressed systemin-mediated**
2 **signaling2 (*spr2*) tomato mutants having impaired mycorrhizal colonization**

4 Kena Casarrubias-Castillo[1], Josaphat M. Montero-Vargas[2], Nicole Dabdoub-González[3], Robert
5 Winkler[4], Norma Martínez-Gallardo[4], Julia Zañudo-Hernández[2], Hamlet Avilés-Arnaut[3]*, John P.
6 Délano-Frier[4]*

8 [1]Centro Universitario de Ciencias Biológicas y Agropecuarias, Universidad de Guadalajara,
9 Nextipac, Zapopan, Jalisco, México
10 [2]Departamento de Investigación en Inmunogenética y Alergia, Instituto Nacional de Enfermedades
11 Respiratorias "Ismael Cosío Villegas", Ciudad de México
12 [3]Instituto de Biotecnología de la Facultad de Ciencias Biológicas, Universidad Autónoma de
13 Nuevo León, Nicolás de los Garza, Nuevo León., México
14 [4]Departamento de Biotecnología y Bioquímica, Centro de Investigación y de Estudios Avanzados
15 del IPN, Unidad Irapuato, Irapuato, Guanajuato, México
16
17
18
19
20
21
22 Corresponding authors:
23 John P. Délano-Frier
24 Telephone: (52) 462 6239636, 462 6239600
25 e-mail: jdelano@ira.cinvestav.mx
26
27 Hamlet Avilés-Arnaut
28 Telephone: (52) 81 8332-0458
29 e-mail: hamlet.avilesarn@uanl.edu.mx
30

33 **ABSTRACT**

34 Arbuscular mycorrhizal fungi (AMF) colonization, sampled at 32 to 50 days post-inoculation

35 (dpi), was significantly reduced in *Suppressor of prosystemin-mediated responses2* (*spr2*) mutant

36 tomato plants impaired in the *ω-3 FATTY ACID DESATURASE7* (*FAD7*) gene that limits the

37 generation of linolenic acid and, consequently, the wound-responsive jasmonic acid (JA) burst.

38 Contrary to wild-type (WT) plants, JA levels in root and leaves of *spr2* mutants remained

39 unchanged in response to AMF colonization, further supporting its regulatory role in the AM

40 symbiosis. Decreased AMF colonization in *spr2* plants was also linked to alterations associated

41 with a disrupted FAD7 function, such as enhanced salicylic acid (SA) levels and SA-related

42 defense gene expression and a reduction in fatty acid content in both mycorrhizal *spr2* roots and

43 leaves. Transcriptomic data revealed that lower mycorrhizal colonization efficiency in *spr2*

44 mutants coincided with the modified expression of key genes controlling gibberellin and ethylene

45 signaling, brassinosteroid, ethylene, apocarotenoid and phenylpropanoid synthesis, and the wound

46 response. Targeted metabolomic analysis, performed at 45 dpi, revealed augmented contents of L-

47 threonic acid and DL-malic acid in colonized *spr2* roots which suggested unfavorable conditions

48 for AMF colonization. Additionally, time- and genotype-dependent changes in root steroid

49 glycoalkaloid levels, including tomatine, suggested that these metabolites might positively

50 regulate the AM symbiosis in tomato. Untargeted metabolomic analysis demonstrated that the

51 tomato root metabolomes were distinctly affected by genotype, mycorrhizal colonization and

52 colonization time. In conclusion, reduced AMF colonization efficiency in *spr2* mutants is probably

53 caused by multiple and interconnected JA-dependent and independent gene expression and

54 metabolomic alterations.

57 **Abbreviations:** AMF, arbuscular mycorrhizal fungi; JA, jasmonic acid; MeJA, methyl jasmonate;

58 SA, salicylic acid; *spr2, Suppressor of prosystemin-mediated response2.*

59 **INTRODUCTION**

60 The roots of the majority of higher plants, and many other host plants including pteridophytes, a

61 number of mosses, lycopods, and psilotales are associated symbiotically with biotrophic and

62 aseptate filamentous fungi of the Glomeromycota phylum, the so-called arbuscular mycorrhizal

63 fungi (AMF) (Redecker and Raab, 2006; Schüssler et al., 2001; van der Heijden et al., 2015). An

64 important feature of the AM symbiosis is the nutrient exchange between both partners, which

65 occurs within individual cortical cells, where AMF form highly branched hyphae, called

66 arbuscules, surrounded by a plant derived periarbuscular membrane. This structure has a unique

67 transport protein distribution designed to deliver mineral nutrients to the cortical cell in exchange

68 for the 4-to-20% of the photosynthates allocated to the roots and subsequently transferred to the

69 fungal symbiont (Gutjahr and Parniske, 2013; Bhandari and Garg, 2017; Rich et al., 2017).

70

71 The mineral exchange principally involves phosphorus (P), although zinc and copper are also

72 thought to be mobilized. AMF substantially enhance P availability to plants considering that this

73 element is mostly found as orthophosphate ions in the soil, which become very poorly mobile in

74 the presence of Ca^{2+}, Fe^{3+} and Al^{3+} (Wang et al., 2017). P uptake relies on phosphate transporters

75 belonging to the phosphate transporter 1 (Pht1) family (Rausch et al., 2001). AMF are also believed

76 to represent a significant route of nitrogen (N) uptake by the plants (Délano-Frier and Tejeda-

77 Sartorius, 2008). In addition to improving plant nutrition and water uptake, root colonization by

78 AMF confers fitness benefits to the host plants. Among these are enhanced root growth and

79 significant changes in root architecture that increase their surface area in the soil and enhance water

80 and nutrient acquisition by the plants. Other benefits include increased reproductive success and/

81 or tolerance to (a)biotic stresses. Several of the above effects are finely regulated by

82 phytohormones, via a limitedly understood and highly context dependent interaction (Gutjahr,

83 2014; Selosse et al., 2014; Pozo et al., 2015; Lenoir et al., 2016; Bedini et al., 2018; Liao et al.,

84 2018; Cabral et al., 2019; Evelin et al., 2019).

85 AMF colonization has been found to profoundly alter gene expression in roots of several plants

86 species (Guimil et al., 2005; Fiorilli et al., 2009; Guether et al., 2009; Hogekamp and Kuester,

87 2013; Groten et al., 2015), whereas a number of large-scale gene expression studies have explored

88 the systemic effects that AMF root colonization has in plant aerial tissues (Guimil et al., 2005;

89 Cervantes-Gamez et al. 2016; Adolfsson et al., 2017; Wang et al., 2018a). Changes in root and leaf

90 metabolite levels in response to AMF colonization, have been also reported, particularly affecting

91 amino acid (aa), carbohydrate and organic acid contents (Schweiger et al., 2014; Rivero et al.,

92 2015; Schweiger and Müller, 2015; French, 2017; Bedini et al., 2018; Wang et al., 2018a).

93

94 Jasmonic acid (JA), its methyl ester (MeJA) and its aa conjugates such as JA-isoleucine,

95 collectively referred as jasmonates, are involved in multiple plant developmental and growth

96 processes, activation of secondary metabolism and defense responses against insects and

97 pathogens in various plant species (Wasternack and Hause, 2013; Erb et el., 2012; Ahmad et al.,

98 2016; Larrieu and Vernou, 2016). JA is biosynthesized through the octadecanoid pathway, being

99 the final product of a series of reactions initiated by the peroxidation of linolenic acid, a C18: 3

100 unsaturated fatty acid (Schaller et al., 2005). Recent models indicate that JA is the long-distance

101 systemic wound signal in tomato. Wound-induced systemic signaling appears to be facilitated by

102 a positive amplification loop in which systemin, a wound related bioactive peptide signal, is

103 considered to play a crucial role (Schilmiller and Howe 2005; Sun et al., 2011). Experimental

104 evidence gathered so far portrays a contradictory role for JA in the regulation of the mycorrhizal

105 symbiosis (Liao et al., 2018; Pozo et al., 2015). While some findings have led to the proposal of

106 several mechanisms designed to explain how JA might positively regulate the AM symbiosis

107 (Isayenkov et al., 2005; Stumpe et al., 2005; Tejeda-Sartorius et al., 2008), others have reported

108 reduced or null effects on AMF colonization in tomato plants treated with exogenous MeJA or in

109 tomato and rice mutants unable to sense or synthesize JA (Herrera-Medina et al., 2008; Gutjahr

110 and Paszkowski, 2009; Gutjahr et al., 2015; Bedini et al., 2018). Additionally, it has been

111 suggested that JA signaling might differentially affect AMF colonization and development by

112 performing different roles in early and late stages of colonization (Foo et al., 2013).

113 Additional findings, derived from the use of the *spr2* tomato mutant as an experimental model

114 (Howe and Ryan, 1999) are reported in this work. The *spr2* tomato mutant is affected in a

115 chloroplast FAD7 fatty acid desaturase that catalyzes the ω3 desaturation of linoleic acid (C18:2)

116 to linolenic acid, JA's biosynthetic precursor. It is also impaired in the wound-induced

117 accumulation of JA and also in the developmentally regulated JA burst in flowers (Li et al., 2002,

118 2003). In addition, the disrupted function of FAD7 has been found to enhance plant defense against

119 aphids due to increased SA levels and SA-related defense gene expression (Avila et al., 2012). The

120 precise mechanism responsible for this effect remains undefined, although direct and indirect

121 FAD7-mediated modulation of SA biosynthesis in the chloroplast has been proposed, the latter via

122 the accumulation of reactive oxygen species (ROS).

123 The results derived from the present study provide congruent arguments to explain how mutant

124 plants negatively affected in the wound-induced accumulation of JA and the subsequent wound-

125 response, are also disrupted in their ability to establish an efficient AM symbiosis. For this purpose,

126 wild-type (WT) and *spr2* plants were analyzed to measure changes in gene expression and

127 metabolic profiles in response to AMF colonization at various sampling points. The results

128 obtained suggest that deficient mycorrhization in *spr2* tomato roots was caused by several factors.

129 Many could be related to physiological changes directly related to the *FAD7* mutation, such as

130 increased SA levels and activation of SA-related gene expression in addition to an alteration in

131 fatty acid composition and abundance in leaves and roots. Indirect effects, occurring as a

132 consequence of the mutant´s inability to undergo mycorrhizal-induced JA accumulation in roots,

133 could have contributed to alter the expression of key genes known to influence AMF colonization,

134 via phytohormone biosynthesis and signaling, in addition to the regulation of the wound-response

135 and of secondary metabolism. In this respect, differential time- and genotype-dependent changes

136 in tomatine, its biosynthetic precursors and catabolic products, in mycorrhizal WT and *spr2* roots,

137 suggested a role of this defense-related metabolite in the regulation of the AM symbiosis. These

138 results are discussed further in the context of the numerous and interconnected mechanisms that

139 control colonization of plants by AMF.

140 **MATERIALS AND METHODS**

141 **Plant Growth and AMF Inoculation**

142 Seeds of wild-type (WT) tomato (*Solanum lycopersicum* L. cv. Castlemart) and *spr2* mutant plants

143 were surface-sterilized by soaking in a 70% ethanol solution for 60 s, with a 20% household bleach

144 solution (5% w/ v sodium hypochlorite) for 5 min, and then rinsed three times with sterile water.

145 All seeds were germinated in a sterile soil mixture constituted by equal parts of sand and loam

146 which was autoclaved six times. One-week-old seedlings were removed and transplanted to 1.3 L

147 pots (one plant per pot, ten plants per genotype) containing the same sterilized soil mixture. At the

148 time of transplanting, ten plants per genotype were inoculated with 3 g of a soil-based (1: 1 sand-

149 loam) inoculum containing ca. 100 AMF spores per g. In the first [E1] of a series of three

150 experiments, performed between April- May 2016, the plant´s inoculum was *Rhizophagus*

151 *irregularis* (*Biofertilizante*, INIFAP, México), whereas in two subsequent ones [E2 and E3,

152   performed between early April-late May and late May- early July 2019, respectively], a consortium

153   of six AMF species, i.e. *Glomus fasciculatus, G. constrictum, G. tortuosum, G. geosporum,*

154   *Gigaspora margarita*, and *Acaulospora scrobicurata* (MycoRacine_VA, MycoBiosfera, México),

155   was used. Similar number of control plants were supplied with 3 g of sterilized soil mixture only.

156   The inoculated and control plants were watered 3 times per week and fertilized once a week with

157   a Long Asthon solution in which the P content was reduced to 7 µM (75% lower than that in the

158   full strength solution), until harvest. They were kept in a growth room with a 16 h/ 8 h light/ dark

159   photoperiod at 27°C (light) and 23°C (dark) with an illumination of approximately 250 µmol m^{-2}

160   s^{-1}. Roots were harvested at different time points: at 50 [E1], 45 [E2] or 32 [E3] days post-

161   inoculation (dpi). The root system was split lengthways at harvest: one half was stained to evaluate

162   mycorrhizal colonization, whereas the remaining root and leaf tissues were frozen, ground in liquid

163   nitrogen, stored at -80°C until required for further analysis.

164   **Estimation of AMF Root Colonization**

165   To evaluate mycorrhizal colonization, root fragments of control and mycorrhized plants (120 per

166   genotype) were stained with trypan blue (Phillips and Hayman, 1970) and observed with a light

167   microscope. AMF colonization was determined in the three independent experiments using two

168   methods: E1 was analyzed as described by Trouvelot et al., (1986) using MYCOCALC software

169   (www2.dijon.inra.fr/ mychintec/ Mycocalc-prg/ download.html), while E2 and E3 were analyzed

170   using the magnified intersections method described by McGonigle et al. (1990). Three

171   colonization parameters were analyzed in E1: frequency of mycorrhization (F%), representing the

172   percentage of root segments showing internal colonization; intensity of mycorrhization (M%), the

173   average percentage of colonization of root segments, and arbuscule abundance (A%), the

174   percentage of arbuscules in the whole root system. In E2 and E3, AMF colonization levels were

175   determined by quantifying the proportion of root length segments containing arbuscules, vesicles

176   and/ or hyphae, each representing the arbuscular (A), vesicular (V) and hyphal colonization (H)

177   levels, respectively.

178   Additionally, physiological parameters such as plant height and changes in chlorophyll content

179   were measured during the duration of the E2 experiment. In addition, maximal photochemical

180   efficiency (*Fv/Fm*) and the photosynthetic potential Index (PI$_{abs}$) were measured as indirect

181   indicators of the quantum efficiency of photosystem II. Chlorophyll content was measured using

182   a CCM-200 plus Chlorophyll Content Meter (Opti-Sciences Inc., Hudson, NH, USA). Fv/Fm and

183   PI_{abs} were determined from data recorded with a portable Pocket PEA chlorophyll fluorometer

184   (Hansatech Instruments LTD; Norfolk, UK). All photosynthesis-related measurements were

185   consistently done at noon.

186   **Determination of jasmonic acid (JA), salicylic acid (SA) and SA conjugates.**

187   JA levels were determined by GC-MS using the methodology described by Muller and Brodschelm

188   (1994). Free SA and SA conjugates were also analyzed by GC-MS, as described by Malamy et al.

189   (1992).

190   **Targeted metabolite profiling and direct fatty acid (FA) analysis by gas chromatography-**

191   **mass spectrometry**

192   The GC-MS targeted metabolite analysis of leaf and root samples was performed according to

193   Eloh et al. (2016). *In situ* FA analysis was done as described by Park and Goins (1994), with slight

194   modifications. These consisted of increasing the 10 min-each methanolysis and methylation steps

195   to 60 and 30 min, respectively. Raw GC-MS data are available from Zenodo (https://zenodo.org/),

196   DOI: 10.5281/zenodo.3560965.

197   **Sample Preparation for Untargeted Metabolomic Analyses**

198   Frozen tomato roots of control and mycorrhizal plants, respectively, were lyophilized and finely

199   ground in a Mixer Mill MM 400 (Retsch GmbH, Haan, Germany) for 12 s at 30 Hz. Subsequently,

200   25 mg of plant powder was extracted with 1 mL of an aqueous methanol-formic acid solution (75%

201   *v/ v* and 0.15% *v/ v*, respectively). The mixture was sonicated for 15 min in a water bath at

202   maximum frequency and centrifuged at $10,000 \times g$ for 10 min at 4°C. The supernatants were

203   filtered through a 0.22 μm syringe filter prior to analysis by mass spectrometry (see below). All

204   samples were freshly prepared in triplicate.

205   **Metabolic Fingerprinting of Tomato Root and Leaf Extracts by Mass Spectrometry**

206   For non-targeted metabolite profiling, tomato root methanolic extracts were analyzed by direct

207   liquid introduction electrospray ionization/ mass spectrometry (DLI-ESI-MS) as described before

208   (Montero-Vargas et al., 2013). Measurements were performed using an ion trap mass spectrometer

209   LCQ-Fleet (Thermo Scientific, USA) in positive mode at a flow rate of 10 μL min^{-1}. Mass spectra

210   were acquired in continuous mode in a range of 50-1300 *m/z*. The scan time was set to 300 ms

211   with three microscans repeated ten times. The instrument settings were: 3.9 kV source voltage, 35

212   V capillary voltage, 330 °C capillary temperature, 80 V tube lens voltage, 15 arbitrary units (AU)

213   of nitrogen sheath gas and 20 AU of auxiliary gas. Additionally, samples were analyzed to detect

214   specific ions corresponding to α-tomatine, its biosynthetic precursors and catabolic products

215   (Montero-Vargas et al., 2018).

216   **Raw Data Processing and Data Analysis**

217   Raw mass spectrometry data were converted to .mzML format with MSConvert (Chambers et al.,

218   2012). The mass spectrum data were processed in R (http://www.rproject.org) using the package

219   MALDIquant version 1.15 (Gibb and Strimmer, 2012) programed to execute the following tasks:

220   .mzML data import, summary of all scans of each spectrum, smoothing by a Savitzky-Golay filter,

221   peak alignment and peak selection detection. Raw data are available from Zenodo

222   (https://zenodo.org/), DOI: 10.5281/zenodo.3560965. Finally, a comparison matrix (*m/z* values for

223   columns and file names for rows) with the intensity of peaks were exported in *csv* format for

224   statistical analysis, applying binning with a bin width of 1 *m/z* and intensity-based normalization.

225   A total of 367, from more than 1000 ion signals, were used after initial data cleaning steps.

226   Unsupervised techniques were employed to explore the effect of mycorrhizal on the metabolic

227   fingerprints of the genotypes employed. These consisted of a hierarchical clustering (HCA) and a

228   principal component Analysis (PCA), both implemented in ClustVis (Metsalu and Vilo, 2015).

229   For multiple comparison of the means a Tukey's Honest Significant Difference (HSD) was applied

230   with a confidence interval of 95 %. When the normality of the data was not achieved, the Kruskal-

231   Wallis test was applied, considering *p* values ≤ 0.05 as significant.

232   For putative metabolite identification, a homebuilt metabolite database for tomato was created

233   based on previous reports (Moco et al., 2006; Itkin et al., 2011; Caprioli et al., 2015) and the

234   SolCyc database (http://solcyc.solgenomics.net/). Subsequently, automatic matching of the *m/z* list

235   was performed employing the software SpiderMass (Winkler, 2015).

236   **Extraction of Total RNA, cDNA Preparation and qPCR Analysis**

237   Total RNA was extracted from 100-500 mg of frozen root tissues with the Trizol reagent

238   (Invitrogen, Carlsbad, CA, USA), according to the manufacturer's instructions, with

239   modifications. These consisted of the addition of a salt solution (sodium citrate 0.8 M + 1.2 M

240   NaCl) during precipitation in a 1: 1 *v/v* ratio with isopropanol and further purification with LiCl

241   (8 M) for 1 h at 4°C. All RNA samples were analyzed by formaldehyde agarose gel electrophoresis

242   and visual inspection of the ribosomal RNA bands upon ethidium bromide staining. Total RNA

243   samples (4 μg) were reverse-transcribed to generate the first-strand cDNA using an oligo dT20

244   primer and 200 units of SuperScript II reverse transcriptase (Invitrogen). The cDNA employed for

245   the qRT-PCR assays was initially prepared from 4 μg total RNA. It was then diluted 5-fold in

246   sterile deionized-distilled (dd) water prior to qRT-PCR. Amplifications were performed using

247   SYBR Green detection chemistry and run in triplicate in 96-well reaction plates with the CFX96

248   Touch Real-Time PCR Detection System (Bio-Rad, Hercules, CA, USA). Reactions were prepared

249   in a total volume of 20 μl containing: 2 μl of template, 2 μl of each amplification primer (2 μM),

250   8 μl of iQ SYBR Green supermix (Bio-Rad) and 6 μl of sterile dd water. Quantitative real-time

251   PCR was performed in triplicate for each sample using the primers listed in the Table S1. Primers

252   were designed for each gene, based on cDNA sequences derived from the tomato genome (Sol

253   Genomics Network; Mueller et al., 2005). Primer design was performed using DNA calculator

254   software (Sigma-Aldrich; St. Louis, MO, USA). The following protocol was followed for all qRT-

255   PCR runs: 15 min at 95°C to activate the JumpStart Taq Polymerase (Sigma-Aldrich), followed

256   by 40 cycles of denaturation at 95°C for 15 s and annealing at 60°C for 1 min. Slow amplifications

257   requiring an excess of 32 cycles were not considered for analysis. The specificity of the amplicons

258   was verified by melting curve analysis after 40 cycles. Baseline and threshold cycles (Ct) were

259   automatically determined using CFX Manager Software version 2.1. PCR efficiencies for all genes

260   tested were greater than 95%. The effect of genotype (WT *vs.* s*pr2*) and treatment (mycorrhizal

261   *vs.* non-mycorrhizal) on the expression of a battery of selected genes was calculated using the 2^{-}

262   $^{\Delta Ct}$ method (Livak and Schmittgen, 2001). Transcript abundance data were normalized against the

263   average transcript abundance of two reference genes: *TIP41* and *SAND* (Expósito-Rodríguez et

264   al., 2008). Values reported are those of 3 independent mycorrhization experiments each one of

265   which was analyzed using mRNA extracted from a single pooled sample prepared by combining

266   the roots of all 10 plants used per experiment. Gene expression data represent the mean ± SE of

267   three technical replicates per combined root pool per independent experiment. qPCR raw data are

268   available from Zenodo (https://zenodo.org/), DOI: 10.5281/zenodo.3560410.

269   **Statistical Analysis of Mycorrhizal Colonization Experiments**

270   Data were analyzed by one-way ANOVA to determine whether or not the means of the different
271   treatments tested were equal. A multiple comparison procedure with the Tukey's test was
272   performed to find significant differences between means. All tests were conducted using the
273   Minitab 15 statistical software package (Minitab Inc., USA). Differences at $p < 0.05$ were
274   considered as statistically significant.

275   **RESULTS**

276   **Mycorrhizal colonization is compromised in *spr2* mutants**

277   Three independent experiments were performed. AMF colonization parameters, irrespective of the
278   AMF used as inoculum and method employed to evaluate colonization, were significantly higher
279   in roots of WT plants compared to *spr2* mutants. The AMF colonization parameters of two
280   independent experiments sampled at 32 days after inoculation (dpi) (E3; Figure 1a) and 45 dpi
281   (E2; Figure 1b), were determined using the magnified intersections method (McGonigle et al.,
282   1990). They were very similar to those of a previous experiment, sampled at 50 dpi (E1), in which
283   AMF colonization was determined using the MYCOCALC software (Figure S1). Apart from the
284   gene expression analysis, all subsequent data was obtained from leaf and root tissues derived from
285   the E2 and E3 experiments.

286   Similar to a previous characterization of the *spr2* tomato mutant (Li et al., 2003), no significant
287   differences in the the growth rate and morphology of *spr2* and WT plants were observed during
288   the experiments herewith described. However, measurement of physiological parameters during
289   the course of E2, indicated that mycorrhizal colonization promoted plant growth, determined as
290   plant height, in WT plants. No growth promotion was recorded in *spr2* plants (Table S2).
291   Irrespective of the genotype, photosynthetic parameters were not altered by mycorrhizal
292   colonization. However, contrary to reported data (Zare-Maivan et al., 2017), AMF colonization
293   had a contrasting effect on chlorophyll content; the significant increase detected in leaves of
294   mycorrhizal *spr2* plants was opposite to the tendency toward lower chlorophyll content observed
295   in equivalent WT leaves (Table S2).

296

297   **Mycorrhizal-induced changes in jasmonic (JA) and salicylic acid (SA) content in leaf and**
298   **roots**

299   JA and SA levels were measured in leaves and roots of plants sampled at 45 dpi. At this sampling
300   point, significantly increased JA contents were detected in both leaves and roots of mycorrhizal

301   WT plants. The effect was more pronounced in leaves. No increase in JA content was produced in

302   equivalent organs of mycorrhizal *spr2* plants (Figures 2a and 2b). Mycorrhizal colonization had

303   no effect on SA levels in roots and leaves of WT. SA content in leaves of *spr2* plants was lower

304   than WT plants and was not modified by AMF colonization, while a significant increase in SA

305   levels was detected in mycorrhizal *spr2* roots (Figures 2c and 2d). No SA-glycosides were

306   detected.

307   **Gene expression profiles**

308   In WT and *spr2* roots, AMF colonization led to several changes in the expression levels of a

309   selected set of genes, which were analyzed at 32, 45 and 50 dpi (Table 1). In general, changes in

310   gene expression were more intense and frequent in roots analyzed at 32 dpi and tended to decrease

311   as the mycorrhizal colonization period extended from 45 to 50 dpi. The gene expression profiles

312   obtained were the following:

313   *Phosphate transporter LePT4*

314   *LePT4* is considered a reliable indicator of mycorrhizal-colonization in roots of *Medicago*

315   *truncatula* and rice (Javot et al., 2007; Wang et al., 2017). In tomato, AMF colonization also

316   induced the accumulation of *LePT4* transcripts. Unexpectedly, *LePT4* expression was higher in

317   mycorrhizal *spr2* roots sampled at 32 and 45 dpi having significantly reduced colonization levels.

318   Irrespective of the genotype, *LePT4* transcript abundance decreased ca. 3-fold in mycorrhizal roots

319   sampled at 45 dpi. This pattern was reversed at 50 dpi, time at which the *LePT4* expression levels

320   coincided with the degree of AMF colonization intensity.

321

322   *Phytohormone-related genes*

323   The expression of three genes involved in brassinosteroid (BR) biosynthesis was mostly repressed

324   in mycorrhizal WT roots, contrary to the widespread induction observed in colonized *spr2* roots.

325   Except for slight variations, the expression pattern was similar in roots harvested at 32, 45 and 50

326   dpi. The genes in question were *DE-ETIOLATED 2* (*DET2*) coding for a steroid 5a-reductase

327   active in the early steps of the BR biosynthetic pathway (Wei and Li, 2016), *DWARF4* (*DWF4*)

328   and *CONSTITUTIVE PHOTOMORPHOGENESIS AND DWARFISM* (*CPD*), both coding for

329   P450 enzymes involved in downstream BR biosynthesis steps (Wei and Li, 2016).

330   The *ENT-COPALYL DIPHOSPHATE SYNTHASE* (*CPS*) and *ENT-KAURENE SYNTHASE* (*KS*)

331   genes code for enzymes catalyzing the initial steps in the gibberellin (GA) biosynthetic pathway

332   leading to the synthesis o*f ent*-kaurene from geranyl-geranyl pyrophosphate in the chloroplast. The

333   *GA 3-OXIDASE* (*GA3ox*) gene codes for an enzyme catalyzing the final steps in the formation of

334   the biologically active GAs, consisting of a series of 3β-hydroxylations of GA-precursors (Hedden

335   and Thomas, 2012). Except for *KS*, downregulated at 32 and 50 dpi in WT mycorrhizal roots, both

336   *CPS* and *GA3ox* tended to be induced in AMF-colonized roots, irrespective of the genotype. On

337   the other hand, the expression of the *GIBBERELLIC ACID INSENSITIVE* (*GAI*) gene, coding for

338   a DELLA protein responsible for repressing GA-dependent signaling (Peng et al., 1997;

339   Schwechheimer, 2012) showed contrasting patterns of expression, remaining repressed in

340   mycorrhizal WT roots along all sampling points, whereas it was mostly induced in equivalent *spr2*

341   roots.

342   The induced expression of the two ABA marker genes was similar in mycorrhizal WT and *spr2*

343   roots sampled at 50 dpi. These included *9-CIS-EPOXYCAROTENOID DIOXYGENASE 1*

344   (*NCED1*), coding for one of the two tomato NCED enzymes that catalyze a key rate-limiting step

345   of ABA biosynthesis (Martín-Rodríguez et al., 2016) and *ABSCISIC ACID AND*

346   *ENVIRONMENTAL STRESS-INDUCIBLE PROTEIN 14* (*TAS14*), coding for a tomato dehydrin

347   induced by osmotic stress and ABA (Godoy et al., 1994).

348   *Apocarotenoid biosynthesis-related genes*

349   The *CCD7* gene codes for one of the two dioxygenases required for strigolactone biosynthesis, an

350   essential component of the initial plant-AMF communication (López-Ráez et al., 2015). Its

351   expression was steadily induced at 32 to 50 dpi in both WT and *spr2* mycorrhizal roots, although

352   expression levels tended to be higher in mycorrhizal *spr2* roots. The *CCD1b* gene, coding for a

353   carotenoid dioxygenase enzyme involved not only in the biosynthesis of C13/ C14 apocarotenoids,

354   but also in the generation of apocarotenoid cleavage products, such as β-ionone, C_{13} α-ionol and

355   C_{14} mycorradicin at late stages of the symbiosis (López-Ráez et al., 2015) was mostly induced in

356   *spr2* roots, although at lower levels than *CCD7*. It´s expression was widely repressed in

357   mycorrhizal WT roots.

358   *9-LOX and 13-LOX pathway genes*

359   Several emblematic 9-LOX pathway genes were induced to similar levels in response to AMF

360   colonization in mycorrhizal WT and *spr2* roots sampled at 50 dpi. Among the octadecanoid

361   pathway genes leading to JA biosynthesis (Ryan, 2000) that were analyzed, *LIPOXYGENASE D*

362   (*LOXD*) was induced to similar levels in WT and *spr2* mycorrhizal roots at 32 dpi. Its expression

363   was subsequently reduced, particularly in WT mycorrhizal roots sampled at 50 dpi. No

364   mycorrhizal-induced changes between genotypes were detected in the expression of *ALLENE*

365   *OXIDE SYNTHASE* (AOS). In contrast, the *JASMONIC ACID CARBOXYL*

366   *METHYLTRANSFERASE* (*JMT*) and the *JASMONATE ZIM DOMAIN2* (*JAZ2*) genes involved in

367   downstream JA signaling remained up-regulated in mycorrhizal WT roots during all three

368   sampling points examined. JAZ2 is a member of the JAZ family of master regulators of the JA

369   signaling pathway (Chung et al., 2009), while JMT is required for the synthesis of MeJA, an active

370   JA volatile signal (Seo et al., 2001).

371   *Wound-response (WR) genes*

372   Only a few marker genes of the JA-dependent wound response (Ryan, 2000) were induced in

373   mycorrhizal WT roots. These were *PINII*, coding for an emblematic protein inhibitor that was up-

374   regulated at 32 dpi. Others were *PS,* coding for the prosystemin precursor protein, and *PPO* and

375   *CYP2*, two late genes coding for a polyphenol oxidase and a cysteine protease, respectively, that

376   were induced at 50 dpi. All other WR genes were repressed in these roots in at least one sampling

377   time point. The negatively affected genes were *AROGP3*, coding for the JA-regulated tomato

378   polygalacturonase non-catalytic subunit gene (Bergey et al., 1999), *RESPIRATORY BURST*

379   *OXIDASE HOMOLOG1* (*RBOH1*), an early WR gene proposed to contribute to the generation of

380   ROS in wounded plants, *LHA1*, an early WR gene coding for a member of the numerous plasma

381   membrane H$^+$-ATPase gene family in tomato (Schaller and Oecking, 1999; Ryan, 2000; Liu et al.,

382   2016) and *SERINE CARBOXYPEPTIDASE* (*SCP*), another late WR marker gene (Ryan, 2000).

383   Most of these genes, in addition to the late *CYSTEINE PROTEINASE* 2 (*CYP2*) WR marker gene,

384   were induced in *spr2* mycorrhizal roots in at least one sampling time point, principally at 32 dpi.

385

386   *Ethylene (ET) biosynthesis- and signaling-related genes*

387   The *CONSTITUTIVE TRIPLE-RESPONSE4* (*CTR4*) gene, coding for a tomato CTR-like protein

388   that is homologous to an *Arabidopsis* Raf mitogen-activated protein triple kinase that suppresses

389   ET signaling (Adams-Phillips et al., 2004; Wang et al., 2018b) was induced in mycorrhizal WT

390   roots sampled at 50 dpi. Most other ET-related genes were either unaffected or were repressed by

391   AMF colonization in WT roots, i.e., the ET biosynthetic and signaling *1-*

392   *AMINOCYCLOPROPANE-1-CARBOXYLATE SYNTHASE2* (*ACS2*) and *ETHYLENE*

393   *INSENSITIVE2* (*EIN2*) genes, respectively. This was contrary to the widespread induction of the

394   ET biosynthetic genes *1-AMINOCYCLOPROPANE-1-CARBOXYLIC ACID (ACC) SYNTHASE6*

395   (*ACS6*) and *ACC OXIDASE4* (*ACO4*) (Wang et al., 2002), and of genes coding for activators of

396   ET signaling and response such as *EIN2* and *EIN3* (Mata et al., 2018) in mycorrhizal *spr2* roots.

397   Activation/ repression of these genes was recorded primarily in roots sampled at 32 dpi. The

398   induction of the ET-related *ERF1b* transcription factor (TF) gene was recorded in mycorrhizal

399   roots of both WT and *spr2* plants sampled at 50 dpi.

400   *Salicylic acid* (*SA*) *signaling-related genes*

401   SA-related genes were analyzed considering previous findings reporting that the *FAD7* mutation

402   in the *spr2* plants positively modulates SA signaling (Avila et al., 2012). Accordingly, the

403   *PATHOGENESIS-RELATED GENE1* (*PR1*), a SA responsive gene induced in response to

404   pathogens and associated with the hypersensitive response in tomato (Tornero et al, 1997) was

405   induced in mycorrhizal *spr2* roots sampled at 32 dpi, but extensively repressed in mycorrhizal WT

406   roots. However, the *SUPPRESSOR OF SA INSENSITIVITY2* (*SSI2*) gene encoding a stearoyl acyl

407   carrier protein involved in the conversion of stearic acid (C18:0) into oleic acid (C18:1) was

408   induced in mycorrhizal *spr2* roots at 32 dpi, but repressed at 45 dpi. The late repression of this

409   gene could have contributed to reduce oleic acid levels, and concomitantly to increase SA content,

410   as reported previously in Arabidopsis, soybean and other plants (Lim et al., 2017). In addition, the

411   *SA CARBOXYL METHYLTRANSFERASE1* (*SMT*) gene that leads to the formation of volatile

412   methyl salicylate (MeSA), considered to act as a mobile signal for the systemic acquired resistance

413   (SAR) response (Park et al., 2007) and a WRKY transcription factor gene associated with SA

414   signaling (van Verk et al., 2008; Gallou et al., 2012, Li et al., 2019), were induced in mycorrhizal

415   *spr2* roots, generally at 32 dpi. The *SMT* gene was repressed in mycorrhizal WT roots sampled at

416   32 dpi.

417   *Secondary metabolism biosynthetic genes*

418   The analysis of key phenylpropanoid genes indicated that *PAL3* and *PAL4* were widely repressed

419   in mycorrhizal WT roots, whereas they were induced in colonized *spr2* roots sampled at 32 dpi.

420   The expression of *PAL5* was induced by mycorrhizal colonization in WT roots sampled at 50 dpi.

421   These multi-member gene families (Chang et al., 2008), code for enzymes catalyzing the rate-

422   limiting step of the phenylpropanoid biosynthetic pathway responsible for the generation of a high

423   diversity of phenolic substances, including flavonoids. The *FLAVONOL SYNTHASE* (*FLS*) gene

424   coding for an enzyme catalyzing a key step in the synthesis of biologically active flavonols that

425   presumably play a regulatory role in the mycorrhizal symbiosis (Steinkellner et al., 2007; Mandal

426   et al., 2010) was induced in both mycorrhizal WT and *spr2* roots at 50 dpi. The induction of the

427   *1-DEOXY-D-XYLULOSE 5-PHOSPHATE2* (*DXS-2*) gene in mycorrhizal WT roots sampled at 50

428   dpi was positively related to higher AMF colonization. This was consistent with the fact that this

429   gene codes for the critical regulatory enzyme of the plastidial methyl-erythritol-4-phosphate

430   isoprenoid biosynthetic pathway leading to the generation, among many others, of C13-C14

431   apocarotenoid precursors. The *BENZYL ALCOHOL ACETYLTRANSFERASE* (*BEAT*) gene,

432   coding for an enzyme known to participate in synthesis of scent volatiles via benzenoid metabolic

433   pathways (Bera et al., 2017), was also induced only in mycorrhizal WT roots. In contrast, the

434   *FARNESYL-DIPHOSPHATE SYNTHASE1* (*FPS1*) gene, coding for a branch point enzyme of the

435   isoprenoid pathway leading to both sesquiterpenes and sterols, and also considered to be a distal

436   regulatory point of 3-hydroxy-3-methylglutaryl-coenzyme A reductase (HMGR; Szkopiñska,

437   2000), remained unchanged or was repressed at late colonization stages in mycorrhizal WT roots.

438   It was, however, induced in equivalent *spr2* roots at 32 dpi. Two genes involved in the general

439   pathway of steroid biosynthesis leading to phytosterols and the α-tomatine glycoalkaloid (Itkin et

440   al., 2011; Moses et al., 2014, Jin et al., 2017) were tested. *CYCLOARTENOL SYNTHASE* (*CAS1*)

441   was induced in AMF colonized *spr2* roots at 32 and 50 dpi but extensively repressed in equivalent

442   WT roots. A similar expression pattern was shown by the *GLYCOALKALOID METABOLISM 1*

443   (*GAME1*) gene.

444   **Targeted metabolic profile of tomato roots and leaves**

445   The results obtained from a GC-MS analysis designed to detect selected metabolites,

446   predominantly associated with primary metabolism in roots and leaves of control and mycorrhizal

447   tomato plants analyzed at 45 dpi is shown in Tables 2 and 3. Different tendencies in metabolite

448   variation patterns were detected in roots (Table 2). A comparison of the roots of non-mycorrhizal

449   WT and *spr2* plants, showed that metabolite abundance was predominantly higher in roots of *spr2*

450   plants, since 10 of 14 metabolites affected in the mutant were significantly increased in *spr2* roots.

451 Relevant exceptions were glucose, fructose and sucrose. AMF colonization had a positive effect
452 on root metabolite accumulation, considering that in both WT and *spr2* mycorrhizal roots, 10 of
453 12 and 13 significantly impacted metabolites, respectively, were increased in response to AMF
454 colonization. Isocitric was significantly reduced in mycorrhizal roots of both genotypes, while
455 proline ratio was significantly increased in mycorrhizal WT roots but reduced in equivalent *spr2*
456 roots. Those that increased their abundance in mycorrhizal roots of both WT and *spr2* roots were
457 PO_4^{3-}, diethylene glycol, succinic, propanoic, and fumaric organic acids, furanone and L- threonic
458 acid. Differences were minimal between mycorrhizal WT and *spr2* roots. Only the abundance of
459 DL- malic acid and L-threonic acid was found to be significantly different between them, both
460 being higher in AMF-colonized *spr2* roots.
461 Conversely, the abundance of 16/ 31 metabolites was significantly affected in leaves of *spr2*
462 mutant plants compared WT plants (Table 3). Nine of these were decreased and 7 were increased.
463 Relevant differences were the reduction of 2-butenoic acid, D-glucuronic acid, 1-cyclohexene-3,
464 4, 5-1-carboxylic acid, L-threonic acid, PO_4^{3-} and sucrose, while serine, oxoproline and maleic
465 acid increased. Fructose and glucose levels were also higher in *spr2* leaves. Compared to non-
466 mycorrhizal controls, AMF colonization modified the accumulation of 10 foliar metabolites in
467 *spr2* mutant plants, predominantly in a negative way, since only 3 metabolites (i.e., maleic acid,
468 fructose and D-glucuronic acid) showed significantly increased abundance. A comparison of leaf
469 metabolite abundance between mycorrhizal WT and *spr2* plants followed this tendency, since only
470 5 of the 18 metabolites whose abundance significantly differed in response to AMF colonization
471 in these plants, were found to increase in mycorrhizal *spr2* leaves. Apart from fructose, glucose,
472 maleic acid and oxoproline, already mentioned above, glycerol was also among the metabolites
473 that significantly increased their abundance in mycorrhizal *spr2* leaves.

474 **Fatty acids (FAs) in roots and leaves**
475 The C16:2 $\Delta^{7E, 10E}$, hexadecatrienoic acid and parinaric FAs were not detected in roots of both
476 genotypes, whereas compared to leaves of *spr2* plants (see below), C18:3 levels were only reduced
477 2.1-fold in *spr2* roots, while C18:2 levels were only ca. 1.3 higher (Table 4). In WT roots, AMF
478 colonization increased the content of palmitic and elaidic FAs, while iso-methyl C16:0 (15 Me),
479 eicosanoic (20:0), behenic (C22:0) and lignoceric (C24:0) FAs were significantly reduced. Oleic
480 acid was the only FA whose abundance was increased in response AMF colonization in *spr2* roots.
481 A comparison between mycorrhizal WT and *spr2* roots showed that FA content was, in general,

482 significantly higher in WT roots, since 10/ 11 FAs, excepting linoleic acid, were significantly

483 higher in mycorrhizal WT roots.

484 In leaves of WT plants, AMF colonization positively affected the amount of palmitic, the iso-

485 methyl branched C16:0 (14 Me) FA, C16:1 (Δ^{7E}), linoleic, parinaric (C18:4 $\Delta^{9Z,\ 11E,\ 13Z,\ 15E}$), stearic

486 and eicosanoic (C20:0) FAs, but decreased the content of cis- 7, 10, 13 hexadecatrienoic acid

487 (C16:3 $\Delta^{7E,\ 10E,\ 13E}$) and linolenic acid (Table 5). FA composition in *spr2* plants, most

488 predominantly in leaves, accurately reflected the lost functionality of FATTY ACID

489 DESATURASE7, as their levels of polyunsaturated FAs (i.e. C16:3, linolenic and parinaric acids),

490 compared to WT leaves, were considerably reduced (e.g., an approximately 20-fold reduction in

491 linolenic acid) or remained undetected (e.g., 16:3 and parinaric FAs), whereas the content of C16:2

492 $\Delta^{7E,\ 10E}$ and linoleic FAs was between 6- and 12-fold higher. However, only the content of stearic

493 (increased) and palmitelaidic (decreased) FAs was significantly modified by AMF colonization in

494 leaves of *spr2* plants. (Table 5). A comparison between WT and *spr2* mycorrhizal leaves indicated

495 that most FAs detected, except C16:2 $\Delta^{7E,\ 10E}$ and linoleic acid, were significantly more abundant

496 in the former.

497 **Metabolic fingerprinting of tomato roots**

498 Direct liquid introduction electrospray mass spectrometry (DLI-ESI-MS) fingerprints were

499 generated to examine the effect of mycorrhizal colonization on the global metabolic profile in roots

500 of WT and *spr2* mutant plants. PCA analysis of data from 367 significant metabolites identified in

501 roots sampled at 32 and 45 dpi showed that at 32 dpi, the three PCs, representing 39.2% of the

502 variance permitted the separation of roots metabolomes by both treatment and genotype factors

503 (Figures 3a and b). Similar results were obtained with roots sampled from the 45 dpi experiment,

504 where the separation of root metabolomes by treatment and genotype was possible with the three

505 PCs representing 48.8% of the variance (Figures 3c and d). A clear discrimination between

506 genotype (WT, *spr2*), treatment (± AMF) and duration of treatment (32 vs. 45 dpi) was also

507 revealed by the formation of separate clusters in the heat-map generated after HCA using the 100

508 most intense ions (Figure 4).

509 Mass fingerprints were determined for each individual experiment. The results, shown in Tables

510 S3 and S4, represent the putative metabolite ions whose significant change in abundance was

511 associated with higher/ lower AMF colonization levels at 32 and 45 dpi. They reinforced the above

512 findings showing that the effect of AMF colonization on root primary and secondary metabolism

513   was dependent on factors such as genotype and colonization time. They also agreed partially with

514   the concept that AMF colonization efficiency involves changes in the content of several categories

515   of lipids (see above), including lysophospholipids, in addition to phytosteroids (see below),

516   carotenes, phenolic compounds, polyamines, auxins, cytokinins, amino acids and other nitrogen-

517   containing compounds (Akiyama and Hayashi, 2006; Drissner et al., 2007; Floss et al., 2008b,

518   2009; Whiteside et al., 2012; Jiménez-Bremont et al., 2014; Rivero et al., 2015; Bedini et al., 2018;

519   Sánchez-Bel et al., 2018; Liao et al., 2018).

520   A targeted assay focusing on the analysis of the tomatine biosynthetic pathway (Montero-Vargas

521   et al., 2018) was performed. Differences were observed between genotypes and between non-

522   colonized and colonized plants. They were also influenced by the duration of colonization. In

523   general, the content of α-tomatine, its biosynthetic precursors and related catabolites (Figure 5;

524   Tables 6 and 7), was significantly lower in *spr2* mutant roots. This effect was more pronounced in

525   roots sampled at 45 dpi. The influence of mycorrhizal colonization was also time-dependent in

526   WT and *spr2* roots. At 32 dpi, significantly affected tomatine-related metabolites and total SGAs

527   had a lower abundance in colonized *spr2* roots, while this pattern was reversed at 45 dpi (Figure

528   5; Tables 6 and 7). Thus, α-tomatine content, which was significantly reduced in *spr2* roots in

529   response to AMF colonization at 32 dpi, became enhanced at 45 dpi. In mycorrhizal WT roots, α-

530   tomatine and most other SGAs teested remained significantly higher than controls only at 32 dpi

531   (Figures 5a and 5b; Tables 6 and 7).

532   **DISCUSSION**

533   **Discernable biochemical and transcriptional changes occur in *spr2* tomato mutants**

534   **compromised in mycorrhizal colonization in tomato**

535   Tomato *spr2* mutant plants consistently showed reduced AMF colonization (Figures 1 and S1) and

536   consequently were unable to benefit from the growth promotion effect usually produced by the

537   AM symbiosis, as observed in mycorrhizal WT plants (Table S2). Low mycorrhization efficiency

538   in *spr2* plants was also in agreement with prior studies reporting deficient mycorrhization in roots

539   of this mutant plant (Tejeda-Sartorius et al., 2008; Song et al., 2015). They differed, however, from

540   data obtained from the JA-deficient *defenseless-1* tomato plant mutants (Howe et al., 1996) which

541   was found to have increased AMF colonization than WT and prosystemin overexpressing

542   transgenic plants (Formenti and Rasmann, 2019). Lower colonization efficiency in *spr2* roots

543   could have partly resulted from their incapacity to significantly increase JA content above control

544 levels in response to AMF colonization (Figure 2). Since *spr2* mutants are impaired in the

545 orchestration of the JA burst required for the activation of wound- and systemin-related defense

546 responses (Li et al., 2003), it may be argued that AMF promote a long-term maintenance of

547 constitutively higher JA levels as a strategy to ensure efficient root colonization. This is in

548 accordance with different scales of AMF-associated JA accumulation previously reported in

549 various plant models, including tomato (Hause et al., 2007; Hause and Schaarschmidt, 2009;

550 López-Ráez et al., 2010; Sánchez-Bel et al., 2016). A plausible use of this strategy could be to

551 orchestrate a JA-related suppression of immunity responses triggered by microbe-associated

552 molecular patterns in order to enhance a positive plant-microorganism interaction, as previously

553 observed in Arabidopsis roots (Jacobs et al., 2011; Lakshmanan et al. 2012). Incidentally,

554 increased JA levels were also in agreement with the proposed priming of JA-dependent defenses

555 in mycorrhizal plants (Cameron et al, 2013; Sánchez-Bel et al., 2016), a trait that was shown to be

556 abolished in *spr2* mutant plants (Song et al., 2015). These scenarios complement other JA-related

557 phenomena proposed to support mycorrhizal colonization (Hause et al., 2007; Tejeda-Sartorius et

558 al., 2008).

559 An additional condition that could have negatively affected AMF colonization in *spr2* plants was

560 the significant SA accumulation observed in mycorrhizal *spr2* roots (Figure 2). In contrast to a

561 previous report linking SA accumulation with a disrupted ω-3 FATTY ACID DESATURASE7

562 function in this mutant (Avila et al., 2012), SA accumulation above WT levels in *spr2* roots

563 occurred exclusively in response to AMF colonization. Nevertheless, the accumulation of SA in

564 *spr2* roots having deficient AMF colonization was in agreement with copious evidence, in various

565 plant models, linking SA with a negative effect on the mycorrhization process at various stages

566 (Fernández et al., 2014; Liao et al., 2018). This outcome is considered to be a consequence of the

567 primary role played by SA in plant defense against biotrophic microorganisms (Pieterse et al. 2009;

568 Gutjahr and Paszkowski, 2009).

569 AMF colonization coincided with the strong induction of the *LePT4* mycorrhizal marker (Table

570 1). Interestingly, the expression levels of this mycorrhizal colonization marker was found to

571 correlate with AMF colonization efficiency only in experiment E1 (Figure S1), which was the

572 longest (i.e., 50 dpi) and was performed using a single AMF species. Conversely, in E2 and E3,

573 *LePT4* expression levels were inversely correlated with AMF colonization efficiency (Figure 1;

574 Table1). The latter combination was in contradiction with findings that established a specific

575   association between this particular phosphate transporter and a functional AMF mycorrhizal
576   symbiosis in *Lotus japonicus*, *Medicago truncatula*, wheat, and rice (Xu et al., 2007; Gutjahr and
577   Parniske, 2013; Wang et al., 2017; Zhang et al., 2019). The discrepancy between the results
578   obtained in E1 with those of E2 and E3 suggest that the use of an AMF consortium *vs.* a single
579   AMF species and, perhaps, the duration of the colonization period could have been contributing
580   factors to the difference observed. Supporting evidence for this possibility is the observation that
581   mycorrhizal phosphate uptake varies among different AMF species. Also, the AMF conditions
582   established in E2 and E3 were more reminiscent of the dynamics of phosphate uptake in the field,
583   which is assumed to be the combined result of the diverse AMF types that contribute separately to
584   phosphate uptake in response to specific environmental conditions, perhaps similar to those
585   encountered in *spr2* roots (Kobae, 2019). Other possible explanations for this apparent disparity
586   may be the likelihood that LePT4 could not be essential for the establishment of the mycorrhizal
587   symbiosis in tomato, considering that the expression of other P transporter genes (i.e., *LePT3* and
588   *LePT5*) was also found to be induced by AMF colonization (Nagy et al, 2005). In addition,
589   mycorrhizal-specific LjPT4 and MtPT4 phosphate transporters were also regulated by early root
590   responses to phosphate levels in non-mycorrhizal roots (Volpe et al., 2016). Another possibility is
591   that mycorrhizal-specific P transporters might have supplementary functions, as supported by the
592   defensive role against pathogenic fungi or abiotic stress recently assigned to mycorrhizal-specific
593   P transporters in wheat (Zhang et al., 2019) and tomato (Volpe et al., 2018). On the other hand,
594   the ca. 3-fold reduction in *LeTP4* expression kevels that occurred as the colonization period
595   extended from 32 to 45 days, and the complete reversal its expression pattern in mycorrhizal WT
596   and *spr2* roots at 50 dpi (Table 1), was in accordance with the expression of mycorrhizal-specific
597   P transporters in wheat roots, which were found to be induced at different stages of the AMF
598   symbiosis (Zhang et al., 2019).
599   Contrasting AMF colonization in WT and *spr2* roots coincided with the possibility that
600   mycorrhization efficiency was enhanced by the repression of *GAI*. Although this proposal
601   disagrees with the proposed regulatory role played by DELLA repressors of GA signaling during
602   the establishment of AM symbiosis (Yu et al., 2014; McGuiness et al., 2019) it is, nevertheless,
603   consistent with other studies evoking a more dynamic role for GAs during the colonization process.
604   Thus, GA levels are believed to fluctuate widely in order to maintain a balance suitable for both

605   for DELLA stability and proper AMF colonization (Foo et al, 2013; Martín-Rodríguez et al., 2015,

606   2016).

607   BR-related genes were strongly repressed in mycorrhizal WT roots, while they were generally up-

608   regulated in mycorrhizal *spr2* roots. This was also in contradiction with the overall positive

609   influence that BRs had in various plant models, including tomato (Bitterlich et al., 2014a, 2014b;

610   Foo et al., 2016; Tofighi et al., 2017). However, most of this information was obtained using BR-

611   deficient mutants under experimental conditions that may have influenced other plant hormones

612   (e.g., ethylene; Jiroutova et al, 2018), known to affect mycorrhizal colonization. Another possible

613   drawback was that the effect on AMF colonization was revealed only after BR levels were severely

614   reduced (Foo et al., 2013). This scenario reflects the paucity of information regarding the precise

615   role played by BRs during the AMF colonization process (Bedini et al., 2018; McGuiness et al.,

616   2019).

617   ABA-related gene expression patterns indicated that the positive influence exerted by the

618   mycorrhizal colonization on ABA biosynthesis and signaling (Herrera-Medina et al., 2007;

619   Martín-Rodríguez et al., 2016), was not affected in the *spr2* mutant. On the other hand, ET gene

620   expression patterns concurred with ample evidence proposing that ET generally has an inhibitory

621   effect on the AMF colonization (Foo et al., 2013, 2016: Pozo et al., 2015; Gomez Monteiro

622   Fracetto et al., 2017). Thus, the majority of the ET biosynthetic and signaling genes analyzed were

623   induced in mycorrhizal *spr2* roots, predominantly at 32 dpi.

624   Similar to ABA, the positive participation assigned to the 9-LOX oxylipin pathway in the AMF

625   colonization process (López-Ráez et al., 2010; León-Morcillo et al., 2016) was not affected in the

626   *spr2* mutants. A comparable argument could be used regarding the 13-LOX pathway, where key

627   regulatory genes of the metabolism and regulation of jasmonates such as *LOXD*, *AOS1*, *JMT* and

628   *JAZ2*, previously found to be induced in mycorrhizal tomato plants (López-Ráez et al., 2010), had

629   similar expression patterns in both WT and *spr2* mycorrhizal roots. On the other hand, some WR

630   gene expression profiles were contrary to expectancy. Extensively repressed *AROGP* expression

631   in mycorrhizal WT roots was incompatible with the conceived need to partially degrade complex

632   carbohydrates in the extracellular matrix to allow fungal spread and periarbuscular matrix

633   formation (Liu et al., 2003). Also, the induction of the *LHA1* gene in *spr2* roots coupled to its

634   repression in equivalent WT roots, at 32 dpi, appeared to be contrary to the presumed role of H^+-

635   ATPases as activators of secondary transport systems at the symbiotic interfaces in tomato

636 (Rosewarne et al., 2007; Liu et al., 2016) and as mediators phosphate transport and plant growth
637 in *M. truncatula* (Krajinski et al., 2014). However, this function is apparently performed in tomato
638 by LHA2, a distinct H$^+$-ATPase isoform. Thus, *LHA2* transcripts were found to accumulate in
639 mycorrhizal tomato roots, contrary to *LHA1* whose expression was repressed by AMF colonization
640 (Ferrol et al., 2002). These workers hypothesized that the selective down-regulation of *LHA1* could
641 reflect a precise role for this transporter during phosphate uptake in tomato, namely in epidermal
642 cells under non-mycorrhizal conditions. They further argued that this resembled the
643 downregulation of two phosphate transporter genes in mycorrhizal *M. truncatula* roots.

644 The broad repression of *RBOH1* in mycorrhizal WT roots was contrary to the proposed NADPH
645 oxidase-mediated increase of ROS in *M. truncatula* required to facilitate root cortex colonization
646 by AMF arbuscules (Belmondo et al., 2016a, 2016b). The induction of *PS* in *spr2* mycorrhizal
647 roots at 32 dpi was counter to reports showing that mycorrhizal roots of *PS* overexpressing plants
648 yielded significantly higher A% levels than WT roots (Tejeda-Sartorius et al., 2008) and that
649 exogenous systemin promoted pre-symbiotic and early AMF colonization phases in tomato (de la
650 Noval-Pons, 2017a, 2017b). A possible argument to explain these apparent contradictions could
651 be that a suppression of certain JA-dependent WR genes is needed to limit JA-related defense
652 responses in order to allow the proper establishment of the mycorrhizal symbiosis (Gutjahr et al.,
653 2015; Martin et al. 2016). Conversely, the strong repression the *SCP* WR gene in mycorrhizal WT
654 roots could have positively affected AMF colonization efficiency by altering the abundance and
655 activity of secreted proteases, including SCPs that are known to activate defense responses via
656 proteolytic degradation processes (Kohler et al., 2015). Apoplastic SCPs are also known to control
657 the generation of peptide signals critical for proper fungal development within the root (Rech et
658 al., 2013). However, the induction of the JA-inducible *PINII* WR marker gene in both WT and
659 *spr2* mycorrhizal roots at 32 dpi was enigmatic.

660 A ca. 2-fold higher expression level of the *CCD7* gene in mycorrhizal *spr2* roots, compared to
661 equivalent WT roots was observed. Irrespective of this difference, the behavior observed was
662 consistent with most experimental evidence indicating that constant *CCD7* gene activation usually
663 observed during AMF colonization is symptomatic of this enzyme´s involvement, together with
664 CCD1, in the production of AMF-induced C13/C14 apocarotenoids. These include α-inol
665 glucoside, the cyclohexenone blumenol and mycorradicin, considered to be signature regulatory
666 metabolites of the AMF symbiosis at late colonization stages (López-Raez et al., 2015; Hou et al.,

667   2016; Lanfranco et al., 2018; Fiorilli et al., 2019). The contrasting *CCD1b* expression levels

668   observed in WT and *spr2* mycorrhizal roots further suggests that apocarotenoid synthesis via

669   CCD1b was differentially regulated in this mutant plant. This finding reinforced the consensus that

670   further research is required to define how apocarotenoid flux is regulated in plants and how these

671   distinctive chemicals, originating from the same metabolic pathway, interact with other

672   phytohormones to regulate the mycorrhization process (Fiorilli et al., 2019).

673

674   AMF colonization had no effect on the expression of *PAL5*, while it led to the repression of the

675   *PAL3* gene in mycorrhizal WT roots, contrary to the induction of both *PAL3* and *PAL4* genes in

676   mycorrhizal *spr2* roots at 32 dpi. These results also disagreed with consensual findings indicating

677   the positive role played by PAL enzymes in the AMF colonization process (Morandi, 1996), via

678   their crucial function as mediators of the biosynthesis of secondary metabolites that stimulate AMF

679   root colonization (Mandal et al., 2010; Steinkellner et al., 2007). However, the induced expression

680   of the AMF-colonization responsive *FLS* gene, required for flavonol synthesis (Scervino et al.,

681   2005), was unaffected by the *spr2* mutation. This contrasted with the *BEAT* gene, whose

682   expression was ca. 10-fold higher in mycorrhizal WT roots sampled at 50 dpi. This gene could

683   have positively impacted the mycorrhizal process via its negative influence on methyl salicylate

684   synthesis (Bera et al., 2017). Likewise, the ca. 4-fold higher *DXS-2* expression levels detected in

685   mycorrhizal WT roots, was in agreement with the positive role played by this gene in the AMF

686   symbiosis via its key involvement in the MVA isoprenoid biosynthetic pathway leading, among

687   others, to the generation of biosynthetic precursors of the above-mentioned C13 and C14

688   apocarotenoids (Walter et al., 2010; Floss et al. 2008a; Liu et al. 2003; Kuhn et al. 2010).

689   *CAS1* catalyzes the cyclization of 2, 3-oxidosqualene, a precursor of cycloartenol, a key metabolic

690   intermediary in sterol biosynthesis, whereas *GAME1* codes for a galactosyltransferase involved in

691   the synthesis of steroidal α-tomatine (Itkin et al., 2011). Both these genes were induced in *spr2*

692   mycorrhizal roots at 32 dpi, while *CAS1* was widely repressed by AMF colonization in WT roots.

693   A similar expression pattern was produced by the *FPS1*, a gene required for the synthesis of

694   farnesyl diphosphate, an early biosynthetic precursor of sterols and triterpenoids (Abe et al., 1993).

695   These results disagreed, however, with the higher accumulation of tomatine, its biosynthetic

696   precursors and catabolic products in mycorrhizal WT roots, particularly at 32 dpi (Figure 5; Tables

697   6 and 7). They were also incompatible with data showing that downregulation of *GAME1* resulted

698   in an almost 50% reduction in α-tomatine levels in tomato leaves (Itkin et al., 2011). However,

699   *GAME1* silencing was observed to lead to the upregulation of various genes known to be involved

700   in pathogen defense. It also caused severe morphological alterations due to changes in membrane

701   sterol levels. This scenario suggests that α-tomatine and related compounds may contribute to

702   maintain AMF colonization in tomato by limiting certain plant defense-responses. They may also

703   act as a stabilizing factor during AMF colonization through their contribution to the maintenance

704   of plant cell viability and, possibly, to the enrichment of membrane micro-domains that modify

705   the fluidity and dynamics of the plasma membrane in order to favor symbiotic plant interactions

706   (Babiychuk et al., 2008; von Sivers et al., 2019). The above arguments suggest that tomatine and

707   related compounds could be important regulators of AMF symbiosis in tomato. Moreover,

708   tomatine metabolite data obtained in this study coincided with previous reports indicating that

709   tomatine biosynthesis was negatively affected in *spr*2 mutant plants (Montero-Vargas et al., 2018)

710   and with findings showing that resistance to necrotrophic fungal and oomycete diseases in *spr2*

711   mycorrhizal tomato plants, was significantly lower than comparable WT plants due to their

712   reliance on the JA-regulated induced systemic response (Song et al., 2015). It also raised the

713   possibility that impaired α-tomatine accumulation in mycorrhizal *spr2* roots could have been partly

714   responsible for their lower AMF colonization efficiency.

715   Another contributing negative factor could have been the induction of SA-related genes, which

716   occurred almost exclusively at 32 dpi in *spr2* mycorrhizal roots (Table 1). Augmented expression

717   of these genes coincided with the significant accumulation of root SA levels and with the induction

718   of *WRKY60*, coding for a tomato TF, closely related to the *Arabidopsi*s WRKY70. This TF is

719   known to regulate the SA-dependent SAR active against biotrophic fungal pathogens (Bai et al.,

720   2018), and to inhibit JA-ET-responsive defense gene expression (Li et al., 2019). Reduced

721   colonization efficiency also agreed with significantly increased expression levels of the *SAMT*

722   gene, coding an enzyme catalyzing the formation of MeSA, considered to be an important

723   component of the long-distance circuitry needed to establish plant SAR (Park et al., 2007; Shah

724   and Zeier, 2013). The only discrepancy was the induced expression in mycorrhizal *spr2* roots of

725   the *SSI1* gene, coding for a stearoyl acyl carrier protein FAD that converts stearic acid to oleic

726   acid, a fatty acid known to inhibit SA signaling (Kachroo et al., 2008). Perhaps its induction

727   reflected the proposed ability of AMF to modulate SA-related defense signaling. In any case, the

728   reduced mycorrhizal efficiency in *spr2* roots having induced levels of SA-related genes

729   corroborated the above mentioned notion that SA acts as an inhibitor of the mycorrhizal symbiosis

730   (Blilou et al., 1999; Herrera-Medina et al., 2003; Bedini et al., 2018).

731   **Differential fatty acid composition and accumulation patterns in leaves and roots could**

732   **contribute to the contrasting AMF colonization levels observed in WT and *spr2* plants**

733   A significantly lower content of mostly all FAs except linoleic acid, was detected in mycorrhizal

734   *spr2* leaves and roots. This key biochemical modification could have contributed to the lower

735   mycorrhization efficiency that characterizes *spr2* plants. The increased levels of palmitic acid and

736   a tendency towards higher oleic in mycorrhizal WT roots acid were relevant in the context of the

737   AMF symbiosis. First, augmented palmitic acid in WT mycorrhizal leaves and roots agreed with

738   recent evidence showing that the AM symbiosis increases the lipid flux and redirects it to generate

739   16:0 β-monoacylglycerols, which are later transferred from the plant to the periarbuscular apoplast

740   (MacLean et al., 2017). Additionally, higher oleic acid in mycorrhizal WT roots, may have favored

741   mycorrhizal colonization by inhibiting SA signaling (Kachroo et al., 2004).

742   Lower FA content in *spr2* mycorrhizal leaves and roots suggested that the C supply to the

743   mycorrhizal fungi, recently demonstrated to be composed by both lipids and sugars (Jiang et al.,

744   2107; Luginbuehl et al., 2017; Roth and Paszkowski, 2017) was probably an additional factor

745   responsible for lower colonization efficiency in *spr2* roots. It remains to be defined if the absence

746   of polyunsaturated 16:3 and 18:3 FAs in *spr2* leaves and roots could have also affected the

747   establishment of AMF by altering the fluidity and/ or transport capacity of their plant cell

748   membranes, including the periarbuscular membrane. This change could have indirectly affected P

749   transport across membranes, or even *spr2* plant fitness, considering that low polyunsaturated FA

750   composition in *fad2* Arabidopsis mutants was shown to reduce the mobility of membrane lipids

751   and to concomitantly impair the Na^+/ H^+ pump function and the proton translocating activity of

752   ATPases (Zhang et al., 2012). Also relevant was the relation to data generated by an untargeted

753   metabolomic analysis in tomato that revealed that α-linolenic acid derivatives were positively

754   affected by the mycorrhizal symbiosis (Rivero et al., 2015). Finally, FA data were in accordance

755   with a report showing that, in addition to flavonoids, linolenic acid, and linoleic acid were key

756   factors responsible of regulating AM colonization in litchi trees (Shu et al., 2016).

757   **Differential metabolite accumulation in roots coincided with differential AMF colonization**

758   **in WT and *spr2* plants**

759   A supervised principal component analysis of signals derived from an untargeted metabolomic

760   analysis of root extracts emphasized the variability observed between mycorrhizal roots of WT

761   and *spr2* plants (Figures 3 and 4; Tables S3 and S4). Additionally, a GC-MS targeted metabolic

762   analysis revealed that AMF colonization had a much more pronounced effect on metabolite

763   abundance in leaves than in roots of plants sampled at 45 dpi. The relevant increase in sucrose

764   content, coupled to lowered glucose and fructose levels, in WT mycorrhizal leaves, was in

765   agreement with their increased need to redirect sucrose from leaves to roots to support their higher

766   colonization rates compared to *spr2* plants (Roth and Paszkowski, 2017). A similar argument could

767   explain the significantly higher level of PO_4^{3-} in leaves of mycorrhizal WT leaves. On the other

768   hand, significantly higher content of DL-malic acid and L-threonic acid in *spr2* roots deficient in

769   mycorrhizal colonization could have mirrored a metabolic condition not amenable to AMF

770   colonization (Bedini et al., 2018). With respect to the SA-dependent implementation of the AMF-

771   inhibiting SAR described above, it is germane to add that SA is also believed to involve a

772   repression of fermentation, higher cytosolic oxidative potential and other conditions known to

773   favor AMF colonization (Bedini et al., 2018).

774   **CONCLUSIONS**

775   Root transcriptomic and metabolomic data indicated that reduced AMF colonization in *spr2* roots

776   was likely caused by JA-dependent and JA-independent factors. The latter involved SA

777   accumulation and induction of SA-regulated defense related genes. The differential expression of

778   key GA and ET genes in mycorrhizal WT and *spr2* roots strongly suggested that alterations in the

779   signaling and/ or biosynthetic pathways of these phytohormones were also central to the regulation

780   of the mycorrhizal symbiosis in tomato. This included the positive association observed between

781   augmented JA levels, induced expression of late JA-dependent WR genes and mycorrhizal

782   efficiency. Targeted and untargeted metabolomic analyses of mycorrhizal WT and *spr2* roots

783   indicated that AMF colonization levels led to significant modifications in their respective

784   metabolomes. These included changes in their fatty acid profiles and in certain metabolites

785   associated with a physiological state favorable to the establishment of the AM symbiosis. In this

786   regard, the accumulation of tomatine and related SGAs appeared to positively regulate the

787   mycorrhizal process, particularly at earlier colonization stages.

788   **ACKNOWLEDGEMENTS**

789   We are grateful to Dr. Gregg Howe (Michigan State University) for kindly supplying the *spr2*

790   tomato seeds and the Tomato Genetic Resource Center at the University of California, Davis, for

791   donating the cv. Castlemart tomato seeds.

792

793

794

795

796

797

798

799

800

801

802

803

804

805

806

807

808

809

810

811

812

813

814

815

816

817

818

819   **REFERENCES**

820 Abe I, Rohmer M, Prestwich GD (1993) Enzymatic cyclization of squalene and oxidosqualene to sterols and
821 triterpenes. Chem. Rev. 93: 2189-2206.
822
823 Adams-Phillips L, Barry C, Giovannoni J (2004) Signal transduction systems regulating fruit ripening. Trends Plant
824 Sci. 9: 331-338.
825
826 Adolfsson L, Nziengui H, Abreu IN, Šimura J, Beebo A, Herdean A, Aboalizadeh J, Široká J, Moritz T, Novák O,
827 Ljung K, Schoefs B, Spetea C (2017) Enhanced secondary- and hormone metabolism in leaves of arbuscular
828 mycorrhizal *Medicago truncatula*. Plant Physiol. 175: 392-411.
829
830 Ahmad P, Rasool S, Gul A, Sheikh SA, Akram NA, Ashraf M, Kazi AM, Gucel S (2016) Jasmonates: Multifunctional
831 roles in stress tolerance. Front. Plant Sci. 7: 813.
832
833 Akiyama K, Hayashi H (2006) Strigolactones: chemical signals for fungal symbionts and parasitic weeds in plant
834 roots. Ann. Bot. 97: 925-931.
835
836 Avila CA, Arevalo-Soliz LM, Jia L, Navarre DA, Chen Z, Howe GA, Meng QW, Smith JE, Goggin FL (2012) Loss
837 of function of FATTY ACID DESATURASE 7 in tomato enhances basal aphid resistance in a salicylate-dependent
838 manner. Plant Physiol. 158: 2028-2041.
839
840 Babiychuk E, Bouvier-Navé P, Compagnon V, Suzuki M, Muranaka T, van Montagu M, Kushnir S, Schaller H (2008)
841 Allelic mutant series reveal distinct functions for *Arabidopsis* cycloartenol synthase 1 in cell viability and plastid
842 biogenesis. Proc. Natl. Acad. Sci. USA. 105: 3163-3168.
843
844 Bai Y, Sunarti S, Kissoudis C, Visser RGF, van der Linden CG (2018) The role of tomato *WRKY* genes in plant
845 responses to combined abiotic and biotic stresses. Front. Plant Sci. 9: 801.
846
847 Bedini A, Mercy L, Schneider C, Franken P and Lucic-Mercy E (2018) Unraveling the initial plant hormone signaling,
848 metabolic mechanisms and plant defense triggering the endomycorrhizal symbiosis behavior. *Front. Plant Sci.* 9:
849 1800.
850
851 Belmondo S, Calcagno C, Genre A, Puppo A, Pauly N, Lanfranco L (2016a) NADPH oxidases in the arbuscular
852 mycorrhizal symbiosis. Plant Signal. Behav. 4: e1165379.
853
854 Belmondo S, Calcagno C, Genre A, Puppo A, Pauly N, Lanfranco L (2016b) The *Medicago truncatula MtRbohE* gene
855 is activated in arbusculated cells and is involved in root cortex colonization. Planta 243: 251-262.
856
857 Bhandari P, Garg N, (2017) Dynamics of arbuscular mycorrhizal symbiosis and its role in nutrient acquisition: an
858 overview. In: Varma, A., Prasad, R., Tuteja, N. (Eds.), Mycorrhiza- Nutrient Uptake, Biocontrol, Ecorestoration.
859 Springer, Cham, pp. 21-43.
860
861 Bera P, Mukherjee C, Mitra A (2017) Enzymatic production and emission of floral scent volatiles in *Jasminum*
862 *sambac*. Plant Sci. 256: 25-28.
863
864 Bergey DR, Orozco-Cardenas M, de Moura DS, Ryan CA (1999) A wound- and systemin-inducible polygalacturonase
865 in tomato leaves. Proc. Natl. Acad. Sci. USA 96: 1756-1760.
866
867 Bitterlich M, Krügel U, Boldt-Burisch K, Franken P, Kühn C (2014a) Interaction of brassinosteroid functions and
868 sucrose transporter SlSUT2 regulate the formation of arbuscular mycorrhiza. Plant Signal. Behav. 9: e970426.
869 Bitterlich M, Krügel U, Boldt-Burisch K, Franken P, Kühn C (2014b) The sucrose transporter SlSUT2 from tomato
870 interacts with brassinosteroid functioning and affects arbuscular mycorrhiza formation. Plant J. 78: 887-899.
871

872   Blilou I, Ocampo JA, García-Garrido JM (1999) Resistance of pea roots to endomycorrhizal fungus or *Rhizobium*
873   correlates with enhanced levels of endogenous salicylic acid. J. Exp. Bot. 50: 1663-1668.
874
875   Cabral C, Wollenweber B, António C, Ravnskov S (2019) Activity in the arbuscular mycorrhizal hyphosphere warning
876   neighbouring plants. Front. Plant Sci. 10: 511.
877
878   Cameron DD, Neal AL, Van Wees SCM, Ton J (2013) Mycorrhiza-induced resistance: more than the sum of its parts?
879   Trends Plant Sci. 18: 539-545.
880   Caprioli G, Cahill M, Logrippo S, James K (2015) Elucidation of the mass fragmentation pathways of tomatidine and
881   β 1-hydroxytomatine using orbitrap mass spectrometry. Nat. Prod. Commun. 10: 575-576.
882
883   Cervantes-Gamez RG, Alonso Bueno-Ibarra M, Cruz-Mendivil A, Ligne Calderon-Vazquez C, Maria Ramirez-
884   Douriet C, Eduardo Maldonado-Mendoza I, Angel Villalobos-Lopez M, Valdez-Ortiz A, Lopez-Meyer M (2016)
885   Arbuscular mycorrhizal symbiosis-induced expression changes in *Solanum lycopersicum* leaves revealed by RNA-
886   seq analysis. Plant Mol. Biol. Rep. 34: 89-102.
887
888   Chambers MC, Maclean B, Burke R, Amodei D, Ruderman DL, Neumann S, Gatto L, Fischer B, Pratt B, Egertson J,
889   Hoff K, Kessner D, Tasman N, Shulman N, Frewen B, Baker TA, Brusniak M-Y, Paulse C, Creasy D, Flashner L,
890   Kani K, Moulding C, Seymour SL, Nuwaysir LM, Lefebvre B, Kuhlmann F, Roark J, Rainer P, Detlev S, Hemenway
891   T, Huhmer A, Langridge J, Connolly B, Chadick T, Holly K, Eckels J, Deutsch EW, Moritz RL, Katz JE, Agus DB,
892   MacCoss M, Tabb DL, Mallick P (2012) A cross-platform toolkit for mass spectrometry and proteomics. Nat.
893   Biotechnol. 30: 918-920.
894
895   Chang A, Lim MH, Lee SW, Robb EJ, Nazar RN (2008) Tomato phenylalanine ammonia-lyase gene family, highly
896   redundant but strongly underutilized. J. Biol. Chem. 283: 33591-33601.
897
898   Chung HS, Niu Y, Browse J, Howe GA (2009) Top hits in contemporary JAZ: An update on jasmonate signaling.
899   Phytochemistry 70: 1547-1559.
900
901   Délano-Frier JP, Tejeda-Sartorius M (2008) Unravelling the network: Novel developments in the understanding of
902   signaling and nutrient exchange mechanisms in the arbuscular mycorrhizal symbiosis. Plant Signal. Behav. 3: 936-
903   944.
904
905   Drissner D, Kunze G, Callewaert N, Gehrig P, Tamasloukht M, Boller T, Felix G, Amrhein N, Bucher M (2007) Lyso-
906   phosphatidylcholine is a signal in the arbuscular mycorrhizal symbiosis. Science. 318: 265-268.
907
908   Eloh K, Sasanelli, N, Maxia A, Caboni P (2016) Untargeted metabolomics of tomato plants after root-knot nematode
909   infestation. J. Agric. Food Chem. 64: 5963-5968.
910
911   Erb M, Meldau S, Howe GA (2012). Role of phytohormones in insect-specific plant reactions. Trends Plant Sci. 17:
912   250-259.
913
914   Evelin H, Devi TS, Gupta S, Kapoor R (2019) Mitigation of salinity stress in plants by arbuscular mycorrhizal
915   symbiosis: Current understanding and new challenges. Front. Plant Sci. 10: 470.
916
917   Expósito-Rodríguez M, Borges AA, Borges-Pérez A, Pérez JA (2008) Selection of internal control genes for
918   quantitative real-time RT-PCR studies during tomato development process. BMC Plant Biol. 8: 131.
919
920   Fernández I, Merlos M, López-Ráez JA, Martínez-Medina A, Ferrol N, Azcón C, Bonfante P, Flors V, Pozo MJ
921   (2014) Defense related phytohormones regulation in arbuscular mycorrhizal symbioses depends on the partner
922   genotypes. J. Chem. Ecol. 40: 791-803.
923
924   Ferrol N, Pozo MJ, Antelo M, Azcón-Aguilar C (2002) Arbuscular mycorrhizal symbiosis regulates plasma membrane
925   H$^+$-ATPase gene expression in tomato plants. J. Exp. Bot. 53: 1683-1687.
926

Fiorilli V, Catoni M, Miozzi L, Novero M, Accotto G, Lanfranco L (2009) Global and cell-type gene expression profiles in tomato plants colonized by an arbuscular mycorrhizal fungus. New Phytol. 184: 975 -987.

Fiorilli V, Wang JY, Bonfante P, Lanfranco L, Al-Babili S (2019) Apocarotenoids: Old and new mediators of the arbuscular mycorrhizal symbiosis. Front. Plant Sci. 10: 1186.

Floss DS, Hause B, Lange PR, Kuster H, Strack D and Walter MH (2008a) Knock-down of the MEP pathway isogene *1-deoxy-D-xylulose 5-phosphate synthase 2* inhibits formation of arbuscular mycorrhiza-induced apocarotenoids, and abolishes normal expression of mycorrhiza-specific plant marker genes. Plant J. 56: 86-100.

Floss DS, Schliemann W, Schmidt J, Strack D, Walter MH (2008b) RNA interference-mediated repression of *MtCCD1* in mycorrhizal roots of *Medicago truncatula* causes accumulation of C-27 apocarotenoids, shedding light on the functional role of CCD1. Plant Physiol. 148: 1267-1282.

Floss DS, Walter MH (2009) Role of carotenoid cleavage dioxygenase 1 (CCD1) in apocarotenoid biogenesis revisited. Plant Signal. Behav. 4: 172-175.

Foo E, Ross JJ, Jones WT, Reid JB (2013) Plant hormones in arbuscular mycorrhizal symbioses: an emerging role for gibberellins. Ann. Bot. 111: 769-779.

Foo E, McAdam EL Weller JL, Reid JB (2016) Interactions between ethylene, gibberellins, and brassinosteroids in the development of rhizobial and mycorrhizal symbioses of pea. J. Exp. Bot. 67: 2413-2424.

Formenti L, Rasmann S (2019) Mycorrhizal fungi enhance resistance to herbivores in tomato plants with reduced jasmonic acid production. Agronomy 9: 131.

French KE (2017) Engineering mycorrhizal symbioses to alter plant metabolism and improve crop health. Front. Microbiol. 8: 1403.

Gallou A, Declerck S, Cranenbrouck S (2012) Transcriptional regulation of defence genes and involvement of the WRKY transcription factor in arbuscular mycorrhizal potato root colonization. Funct. Integr. Genomics 12: 183-198.

Gibb S, Strimmer K (2012) MALDIquant : a versatile R package for the analysis of mass spectrometry data. Bioinformatics 28: 2270-2271.

Godoy JA, Lunar R, Torres-Schumann S, Moreno J, Rodrigo RM, Pintortoro JA (1994) Expression, tissue distribution and subcellular-localization of dehydrin Tas14 in salt-stressed tomato plants. Plant Mol. Biol. 26: 1921-1934.

Gomez Monteiro Fracetto G, Pereira Peres LE, Rodriguez Lambais M (2017) Gene expression analyses in tomato near isogenic lines provide evidence for ethylene and abscisic acid biosynthesis fine-tuning during arbuscular mycorrhiza development. Arch. Microbiol. 199: 787-798.

Groten K, Pahari NT, Xu S, van Doorn MM, Baldwin IT (2015) Virus-induced gene silencing using tobacco rattle virus as a tool to study the interaction between *Nicotiana attenuata* and *Rhizophagus irregularis*. Plos One 10: e0136234.

Guether M, Balestrini R, Hannah M, He J, Udvardi M, Bonfante P (2009) Genome-wide reprogramming of regulatory networks, transport, cell wall and membrane biogenesis during arbuscular mycorrhizal symbiosis in *Lotus japonicus*. New Phytol. 182: 200-212.

Guimil S, Chang HS, Zhu T, Sesma A, Osbourn A, Roux C, Ionnidis V, Oakeley EJ, Docquier M, Descombes P, Briggs SP, Paszkowski U (2005) Comparative transcriptomics of rice reveals an ancient pattern of response to microbial colonization. Proc. Natl. Acad. Sci. USA 102: 8066-8070.

Gutjahr C, Paszkowski, U (2009) Weights in the balance: jasmonic acid and salicylic acid signaling in root-biotroph interactions. Mol. Plant-Microbe Interact. 22: 763-772.

982 Gutjahr C, Parniske M (2013) Cell and developmental biology of arbuscular mycorrhiza symbiosis. Ann. Rev. Cell
983 Dev. Biol. 29: 593-617.
984
985 Gutjahr C (2014) Phytohormone signaling in arbuscular mycorhiza development. Curr. Opin. Plant Biol. 20: 26-34.
986
987 Gutjahr C, Siegler H, Haga K, Iino M, Paszkowski U (2015) Full establishment of arbuscular mycorrhizal symbiosis
988 in rice occurs independently of enzymatic jasmonate biosynthesis. PLoS ONE 10: e0123422.
989
990 Hause B, Mrosk C, Isayenkov S, Strack D (2007) Jasmonates in arbuscular mycorrhizal interactions. Phytochemistry
991 68: 101-110.
992
993 Hause B, Schaarschmidt S (2009) The role of jasmonates in mutualistic symbioses between plants and soil-born
994 microorganisms. Phytochemistry 70:1589-1599.
995
996 Hedden P, Thomas SG (2012) Gibberellin biosynthesis and its regulation. Biochem. J. 444: 11-25.
997
998 Herrera-Medina MJ, Gagnon H, Piché Y, Ocampo JA, García Garrido JM, Vierheilig H (2003) Root colonization by
999 arbuscular mycorrhizal fungi is affected by the salicylic acid content of the plant. Plant Sci. 164: 993-998.
1000
1001 Herrera-Medina MJ, Steinkellner S, Vierheilig H, Ocampo JA, García-Garrido JM (2007) Abscisic acid determines
1002 arbuscule development and functionality in the tomato arbuscular mycorrhiza. New Phytol. 175: 554-564.
1003
1004 Herrera-Medina MJ Tamayo MI Vierheilig H, Ocampo JA, Garcia-Garrido JM (2008) The jasmonic acid signalling
1005 pathway restricts the development of the arbuscular mycorrhizal association in tomato. J. Plant Growth Regul. 27:
1006 221-230.
1007
1008 Hogekamp C, Küster H (2013) A roadmap of cell-type specific gene expression during sequential stages of the
1009 arbuscular mycorrhiza symbiosis. BMC Genomics. 14: 306
1010
1011 Hou X, Rivers J, León P, McQuinn RP, Pogson BJ (2016) Synthesis and function of apocarotenoid signals in plants.
1012 Trends Plant Sci. 21: 792-803.
1013 .
1014 Howe GA, Lightner J, Browse J, Ryan CA (1996) An octadecanoid pathway mutant (JL5) of tomato is compromised
1015 in signaling for defense against insect attack. Plant Cell. 8: 2067-2077.
1016
1017 Howe GA, Ryan CA (1999) Suppressors of systemin signaling identify genes in the tomato wound response pathway.
1018 Genetics 153: 1411-1421.
1019
1020 Itkin M, Rogachev I, Alkan N, Rosenberg T, Malitsky S, Masini L, Meir S, Iijima Y, Aoki K, de Vos R, Prusky D,
1021 Burdman S, Beekwilder J, Aharoni A (2011) GLYCOALKALOID METABOLISM1 is required for steroidal alkaloid
1022 glycosylation and prevention of phytotoxicity in tomato. Plant Cell 23: 4507-4525.
1023
1024 Isayenkov S, Mrosk C, Stenzel I, Strack D, Hause B (2005) Suppression of allene oxide cyclase in hairy roots of
1025 *Medicago truncatula* reduces jasmonate levels and the degree of mycorrhization with *Glomus intraradices*. Plant
1026 Physiol. 139: 1401-1410.
1027
1028 Jacobs S, Zechmann B, Molitor A, Trujillo M, Petutschnig E, Lipka V, Kogel K-H, Schäfer P (2011) Broad-spectrum
1029 suppression of innate immunity is required for colonization of Arabidopsis roots by the fungus *Piriformospora indica*.
1030 Plant Physiol. 156: 726-740.
1031
1032 Javot H, Penmetsa RV, Terzaghi N, Cook DR, Harrison MJA (2007) *Medicago truncatula* phosphate transporter
1033 indispensable for the arbuscular mycorrhizal symbiosis. Proc. Natl. Acad. Sci. USA 104: 1720-1725.
1034
1035 Jiang Y, Wang W, Xie Q, Liu N, Liu L, Wang D, Zhang X, Yang C, Chen X, Tang D, Wang E (2017) Plants transfer
1036 lipids to sustain colonization by mutualistic mycorrhizal and parasitic fungi. Science 356: 1172-1175.

Jiménez-Bremont JF, Marina M, Guerrero-González ML, Rossi FR, Sánchez-Rangel D, Rodríguez-Kessler M, Ruiz OA, Gárriz A (2014) Physiological and molecular implications of plant polyamine metabolism during biotic interactions. Front. Plant Sci. 5: 95.

Jin ML, Lee WM, Kim OT (2017) Two cycloartenol synthases for phytosterol biosynthesis in *Polygala tenuifolia* Willd. Int. J. Mol. Sci. 18: E2426.

Jiroutova P, Oklestkova J, Strnad M (2018) Crosstalk between brassinosteroids and ethylene during plant growth and under abiotic stress conditions. Int. J. Mol. Sci. 19: 3283.

Kobae Y (2019) Dynamic phosphate uptake in arbuscular mycorrhizal roots under field conditions. Front. Environ. Sci. 6: 159.

Kohler A, Kuo A, Nagy LG, Morin E[1], Barry KW, Buscot F, Canbäck B, Choi C, Cichocki N, Clum A, Colpaert J, Copeland A, Costa MD, Doré J, Floudas D, Gay G, Girlanda M, Henrissat B, Herrmann S, Hess J, Högberg N, Johansson T, Khouja HR, LaButti K, Lahrmann U, Levasseur A, Lindquist EA, Lipzen A, Marmeisse R, Martino E, Murat C, Ngan CY, Nehls U, Plett JM, Pringle A, Ohm R, Perotto S, Peter M, Riley R, Rineau F, Ruytinx J, Salamov A, Shah F, Sun H, Tarkka M, Tritt A, Veneault-Fourrey C, Zuccaro A; Mycorrhizal Genomics Initiative Consortium, Tunlid A, Grigoriev IV, Hibbett DS, Martin F (2015) Convergent losses of decay mechanisms and rapid turnover of symbiosis genes in mycorrhizal mutualists. Nat. Genet. 47: 410-415.

Kachroo A, Venugopal SC, Lapchyk L, Falcone D, Hildebrand D, Kachroo P (2004) Oleic acid levels regulated by glycerolipid metabolism modulate defense gene expression in Arabidopsis. Proc. Natl. Acad. Sci. USA 101: 5152-5157.

Kachroo A, Fu D-Q, HavensW, Navarre D, Kachroo P, Ghabrial SA (2008) An oleic acid-mediated pathway induces constitutive defense signaling and enhanced resistance to multiple pathogens in soybean. Mol. Plant Microbe Interact. 21: 564-575.

Krajinski F, Courty P-E, Sieh D, Franken P, Zhang H, Bucher M, Gerlach N, Kryvoruchko I, Zoeller D, Udvardi M, Hause B (2014) The H$^+$-ATPase HA1 of *Medicago truncatula* is essential for phosphate transport and plant growth during arbuscular mycorrhizal symbiosis. Plant Cell 26: 1808-1817.

Kuhn H, Küster H, Requena N (2010) Membrane steroid-binding protein 1 induced by a diffusible fungal signal is critical for mycorrhization in *Medicago truncatula*. New Phytol. 185: 716-733.

Lakshmanan V, Kitto SL, Caplan JL, Hsueh Y, Kearns DB, Wu Y, Bais HP (2012) Microbe-associated molecular patterns-triggered root responses mediate beneficial rhizobacterial recruitment in Arabidopsis. Plant Physiol. 160: 1642-1661.

Lanfranco L, Fiorilli V, Venice F, Bonfante P (2018) Strigolactones cross the kingdoms: plants, fungi, and bacteria in the arbuscular mycorrhizal symbiosis. J. Exp. Bot. 69: 2175-2188.

Larrieu A, Vernou T (2016) Q&A: How does jasmonate signaling enable plants to adapt and survive? BMC Biol. 14: 79.

Li, L., Li, C., Lee, G.I., and Howe, G.A. (2002). Distinct roles for jasmonic acid synthesis and action in the systemic wound response of tomato. Proc. Natl. Acad. Sci. USA 99: 6416-6421.

Li C, Liu G, Xu C, Lee GI, Bauer P, Ling HQ, Ganal MW, Howe GA (2003) The tomato *suppressor of prosystemin-mediated responses2* gene encodes a fatty acid desaturase required for the biosynthesis of jasmonic acid and the production of a systemic wound signal for defense gene expression. Plant Cell 15: 1646-1661.

Li N, Han X, Feng D, Yuan D, Huang LJ (2019) Signaling crosstalk between salicylic acid and ethylene/ jasmonate in plant defense: Do we understand what they are whispering? Int. J. Mol. Sci. 20: 671.

Lenoir I, Fontaine J, Sahraoui AL (2016) Arbuscular mycorrhizal fungal responses to abiotic stresses: A review. Phytochemistry 123, 4-15.

Leon-Morcillo RJ, Navarrete MI, Bote JA, Monguio SP, García-Garrido JM (2016) Suppression of allene oxide synthase 3 in potato increases degree of arbuscular mycorrhizal fungal colonization. J Plant Physiol. 190: 15-25.

Liao D, Wang S, Cui M, Liu J, Chen A, Xu G (2018) Phytohormones regulate the development of arbuscular mycorrhizal symbiosis. Int. J. Mol. Sci. 19: 3146.

Lim GH, Singhal R, Kachroo A, Kachroo P (2017) Fatty acid-and lipid-mediated signaling in plant defense. Annu. Rev. Phytopathol. 55: 505-536.

Liu JY, Blaylock LA, Endre G, Cho J, Town CD, VandenBosch KA, Harrison MJ (2003) Transcript profiling coupled with spatial expression analyses reveals genes involved in distinct developmental stages of an arbuscular mycorrhizal symbiosis. Plant Cell 15: 2106-2123.

Liu J, Liu J, Chen A, Ji M, Chen J, Yang X, Gu M, Qu H, Xu G (2016) Analysis of tomato plasma membrane H^+-ATPase gene family suggests a mycorrhiza- mediated regulatory mechanism conserved in diverse plant species. Mycorrhiza 26: 645-656.

Livak KJ, Schmittgen TD (2001) Analysis of relative gene expression data using real-time quantitative PCR and the $2^{-\Delta\Delta Ct}$ method. Methods 25: 402-408.

López-Ráez JA, Kohlen W, Charnikhova T, Mulder P, Undas AK, Sergeant MJ, Verstappen F, Bugg TDH, Thompson AJ, Ruyter-Spira C, Bouwmeester H (2010) Does abscisic acid affect strigolactone biosynthesis? New Phytol. 187: 343-354.

López-Ráez JA, Fernández I, García JM, Berrio E, Bonfante P, Walter MH, Pozo MJ (2015) Differential spatio-temporal expression of carotenoid cleavage dioxygenases regulates apocarotenoid fluxes during AM symbiosis. Plant Sci. 230: 59-69.

Luginbuehl LH, Oldroyd GED (2017) Understanding the arbuscule at the heart of endomycorrhizal symbioses in plants. Curr. Biol. 27: R952-R963.

MacLean A, Bravo A, Harrison MJ (2017) Plant signaling and metabolic pathways enabling arbuscular mycorrhizal symbiosis. Plant Cell. 29: 2319-2335.

Malamy J, Henning J, Klessig DF (1992) Temperature-dependent induction of salicylic acid and its conjugates during the resistance response to tobacco mosaic virus infection. Plant Cell 4: 359-366.

Mandal SM, Chakraborty D, Dey S (2010) Phenolic acids act as signaling molecules in plant-microbe symbioses. Plant Signal. Behav. 5: 359-368.

Martin F, Kohler A, Murat C, Veneault-Fourrey C, Hibbett DS (2016) Unearthing the roots of ectomycorrhizal symbioses. Nat. Rev. Microbiol. 14:760-773.

Martín-Rodríguez JA, Ocampo JA, Molinero-Rosales N, Tarkowská D, Ruíz-Rivero O, García-Garrido JM (2015) Role of gibberellins during arbuscular mycorrhizal formation in tomato: new insights revealed by endogenous quantification and genetic analysis of their metabolism in mycorrhizal roots. Physiol. Plant. 154: 66-81.

Martín-Rodríguez JA, Huertas R, Ho-Plágaro T, Ocampo JA, Turečková V, Tarkowská D, Ludwig-Müller J, García-Garrido JM (2016) Gibberellin-abscisic acid balances during arbuscular mycorrhiza formation in tomato. Front. Plant Sci. 7: 1273.

1146
1147 Mata CI, Fabre B, Parsons HT, Hertog MLATM, Van Raemdonck G, Baggerman G, Van de Poel B, Lilley KS, Nicolaï
1148 BM (2018) Ethylene receptors, CTRs and EIN2 target protein identification and quantification through parallel
1149 reaction monitoring during tomato fruit ripening. Front. Plant Sci. 9: 1626.
1150
1151 McGonigle TP, Miller MH, Evans DG, Fairchild GL, Swan JA (1990) A new method which gives an objective
1152 measure of colonization of roots by vesicular-arbuscular mycorrhizal fungi. New Phytol. 115: 495-501.
1153
1154 McGuiness PN, Reid JB, Foo E (2019) The role of gibberellins and brassinosteroids in nodulation and arbuscular
1155 mycorrhizal associations. Front. Plant Sci. 10: 269.
1156
1157 Metsalu T, Vilo J (2015) Clustvis: a web tool for visualizing clustering of multivariate data using Principal Component
1158 Analysis and heatmap. Nucleic Acids Res. 43(W1): W566-W570.
1159
1160 Moco S, Bino RJ, Vorst O, Verhoeven HA, de Groot J, van Beek TA, Vervoort J, de Vos CHR (2006) A liquid
1161 chromatography-mass spectrometry-based metabolome database for tomato. Plant Physiol. 141: 1205-1218.
1162
1163 Montero-Vargas JM, González-González LH, Gálvez-Ponce E, Ramírez-Chávez E, Molina-Torres J, Chagolla A,
1164 Montagnon C, Winkler R (2013) Metabolic phenotyping for the classification of coffee trees and the exploration of
1165 selection markers. Mol. Biosyst. 9: 693-699.
1166
1167 Montero-Vargas JM, Casarrubias-Castillo K, Martinez-Gallardo N, Ordaz-Ortiz JJ, Delano-Frier JP, Winkler R (2018)
1168 Modulation of steroidal glycoalkaloid biosynthesis in tomato (*Solanum lycopersicum*) by jasmonic acid. Plant Sci.
1169 277: 155-165.
1170
1171 Morandi D (1996) Occurrence of phytoalexins and phenolic compounds in endomycorrhizal interactions, and their
1172 potential role in biological control. Plant Soil 185: 241-251.
1173
1174 Moses T, Papadopoulou KK, Osbourn A (2014) Metabolic and functional diversity of saponins, biosynthetic
1175 intermediates and semi-synthetic derivatives. Crit. Rev. Biochem. Mol. Biol. 49: 439-462.
1176
1177 Muller MJ, Brodschelm W (1994) Quantification of jasmonic acid by gas chromatography-negative chemical
1178 ionization-mass spectrometry. Anal. Biochem. 218: 425-435.
1179
1180 Mueller LA, Solow TH, Taylor N, Skwarecki B, Buels R, Binns J, Lin C, Wright MH, Ahrens R, Wang Y, Herbst
1181 EV, Keyder ER, Menda N, Dani Zamir D, Tanksley SD (2005) The SOL genomics network. A comparative resource
1182 for Solanaceae biology and beyond. Plant Physiol. 138: 1310-1317.
1183
1184 Nagy R, Karandashov V, Chague V, Kalinkevich K, Tamasloukht M, Xu G, Jakobsen I, Levy AA, Amrhein N, Bucher
1185 M (2005) The characterization of novel mycorrhiza-specific phosphate transporters from *Lycopersicon esculentum*
1186 and *Solanum tuberosum* uncovers functional redundancy in symbiotic phosphate transport in solanaceous species.
1187 Plant J. 42: 236-250.
1188
1189 de la Noval-Pons BM, León-Díaz O, Martínez-Gallardo NA, Pérez-Ortega E, Délano-Frier JP (2017a) Pattern of β-
1190 1, 3-glucanase and chitinase activity in the AMF-systemin interaction in tomato. I. Pre-symbiotic phase. Cultivos
1191 Tropicales 38: 36-43.
1192
1193 de la Noval-Pons BM, León-Díaz O, Martínez-Gallardo NA, Pérez-Ortega E, Délano-Frier JP (2017b). Activity
1194 pattern of β-1, 3-glucanases and chitinases in the AMF-systemin interaction in tomato. II. Early symbiotic phase.
1195 Cultivos Tropicales 38: 84-91.
1196
1197 Park PW, Goind RE (1994) *In situ* preparation of fatty acid methyl esters for analysis of fatty acid composition in
1198 foods. J. Food Sci. 59: 1262-1266.
1199

Park SW, Kaimoyo E, Kumar D, Mosher S, Klessig DF (2007) Methyl salicylate is a critical mobile signal for plant systemic acquired resistance. Science 318: 113-116.

Peng J, Carol P, Richards DE, King KE, Cowling RJ, Murphy GP, Harberd NP (1997). The Arabidopsis *GAI* gene defines a signaling pathway that negatively regulates gibberellin responses. Genes Dev. 11: 3194-3205.

Phillips JM, Hayman DS (1970) Improved procedures for cleaning roots and staining parasitic and vesicular-arbuscular mycorrhizal fungi for rapid assessment of infection. Trans. Br. Mycol. Soc. 55: 155-161.

Pieterse CMJ, Leon-Reyes A, Van der Ent S, Van Wees SCM (2009) Networking by small-molecule hormones in plant immunity. Nat. Chem. Biol. 5: 308-316.

Pozo MJ, López-Ráez JA, Azcón-Aguilar C, García-Garrido JM (2015) Phytohormones as integrators of environmental signals in the regulation of mycorrhizal symbioses. New Phytol. 205: 1431-1436.

Rausch C, Daram P, Brunner S, Jansa J, Laloi M, Leggewie G, Amrhein N, Bucher M (2001) A phosphate transporter expressed in arbuscule-containing cells in potato. Nature 414: 462-466.

Rech SS, Heidt S, Requena N (2013) A tandem Kunitz protease inhibitor (KPI106)-serine carboxypeptidase (SCP1) controls mycorrhiza establishment and arbuscule development in *Medicago truncatula*. Plant J. 75: 711-725.

Redecker D, Raab P (2006) Phylogeny of the *Glomeromycota* (arbuscular mycorrhizal fungi): recent developments and new gene markers. Mycologia 98: 885-895.

Rich MK, Nouri E, Courty PE, Reinhardt D (2017) Diet of arbuscular mycorrhizal fungi: bread and butter? Trends Plant Sci. 22: 652-660.

Rivero J, Gamir J, Aroca R, Pozo MJ, Flors V (2015) Metabolic transition in mycorrhizal tomato roots. Front. Microbiol. 6: 598.

Rosewarne GM, Smith FA, Schachtman DP, Smith SE (2007) Localization of proton-ATPase genes expressed in arbuscular mycorrhizal tomato plants. Mycorrhiza 17: 249-258.

Roth R, Paszkowski U (2017) Plant carbon nourishment of arbuscular mycorrhizal fungi. Curr. Opin. Plant Biol. 39: 50-56.

Ryan CA (2000) The systemin signaling pathway: differential activation of plant defensive genes. Biochim. Biophys. Acta. 1477: 112-121.

Sánchez-Bel P, Troncho P, Gamir J, Pozo MJ, Camañes G, Cerezo M, Flors V (2016) The nitrogen availability interferes with mycorrhiza-induced resistance against *Botrytis cinerea* in tomato. Front. Microbiol. 7: 1598.

Sánchez-Bel P, Sanmartín N, Pastor V, Mateu D, Cerezo M, Vidal-Albalat A, Pastor-Fernández J, Pozo MJ, Flors V (2018) Mycorrhizal tomato plants fine tunes the growth-defence balance upon N depleted root environments. Plant Cell Environ. 41: 406-420.

Scervino JM, Ponce MA, Erra-Bassells R, Vierheilig H, Ocampo JA, Godeas A (2005) Flavonoids exclusively present in mycorrhizal roots of white clover exhibit a different effect on arbuscular mycorrhizal fungi than flavonoids exclusively present in non-mycorrhizal roots of white clover. J. Plant Interact. 1: 15-22.

Schaller F, Schaller A, Stintzi A (2005) Biosynthesis and metabolism of jasmonates. J. Plant Growth Regul. 23: 179-199.

Schaller A, Oecking C (1999) Modulation of plasma membrane H1-ATPase activity differentially activates wound and pathogen defense responses in tomato plants. Plant Cell. 11: 263-272.

1255
1256   Schilmiller AL, Howe GA (2005) Systemic signaling in the wound response. Curr. Opin. Plant Biol. 8: 369-377.
1257
1258   Schüssler A, Schwarzott D, Walker C (2001) A new fungal phylum, the *Glomeromycota*: phylogeny and evolution.
1259   Mycol. Res. 105: 1413-1421.
1260
1261   Schwechheimer C (2012) Gibberellin signaling in plants-the extended version. Front. Plant Sci. 2: 107.
1262
1263   Schweiger R, Baier MC, Persicke M, Mueller C (2014) High specificity in plant leaf metabolic responses to arbuscular
1264   mycorrhiza. Nat. Comm. 5: 3886.
1265
1266   Schweiger R, Müller C (2015) Leaf metabolome in arbuscular mycorrhizal symbiosis. Curr. Opin. Plant Biol. 26: 120-
1267   126.
1268
1269   Selosse MA, Bessis A, Pozo MJ (2014) Microbial priming of plant and animal immunity: symbionts as developmental
1270   signals. Trends Microbiol. 22: 607-613.
1271
1272   Seo H, Song J, Cheong JJ, Lee YH, Lee YW, Hwang I, Lee JS, Choi YD (2001) Jasmonic acid carboxyl
1273   methyltransferase: A key enzyme for jasmonate-regulated plant responses. Proc. Natl. Acad. Sci. 98: 4788-4793.
1274
1275   Shah J, Zeier J (2013) Long-distance communication and signal amplification in systemic acquired resistance. Front.
1276   Plant Sci. 4: 30.
1277
1278   Shu B, Li W, Liu L, Wei Y, Shi S (2016) Transcriptomes of arbuscular mycorrhizal fungi and litchi host interaction
1279   after tree girdling. Front. Microbiol. 7: 408.
1280
1281   Song Y, Chen D, Lu K, Sun Z, Zeng R (2015) Enhanced tomato disease resistance primed by arbuscular mycorrhizal
1282   fungus. Front. Plant Sci. 6: 786.
1283
1284   Steinkellner S, Lendzemo V, Langer I, Schweiger P, Khaosaad T, Toussaint JP, Vierheilig H (2007) Flavonoids and
1285   strigolactones in root exudates as signals in symbiotic and pathogenic plant-fungus interactions. Molecules 12: 1290-
1286   1306.
1287
1288   Stumpe M, Carsjens JG, Stenzel I, Göbel C, Lang I, Pawlowski K, Hause B, Feussner I (2005) Lipid metabolism in
1289   arbuscular mycorrhizal roots of *Medicago truncatula*. Phytochemistry 66: 781-791.
1290
1291   Sun JQ, Jiang HL, Li CY (2011) Systemin/ jasmonate-mediated systemic defense signaling in tomato. Mol. Plant 4:
1292   607-615.
1293
1294   Szkopiñska A (2000) Ubiquinone. Biosynthesis of quinone ring and its isoprenoid side chain. Intracellular
1295   localization. Acta Biochim. Pol. 47: 469-480.
1296
1297   Tejeda-Sartorius M, Martínez de la Vega O, Délano-Frier JP (2008) Jasmonic acid influences mycorrhizal
1298   colonization in tomato plants by modifying the expression of genes involved in carbohydrate partitioning. Physiol
1299   Plant. 133: 339-353.
1300
1301   Tofighi C, Khavari-Nejad RA, Najafi F, Razavi K, Rejali F (2017) Brassinosteroid (BR) and arbuscular mycorrhizal
1302   (AM) fungi alleviate salinity in wheat. J. Plant Nutr. 40: 1091-1098.
1303
1304   Tornero P, Gadea J, Conejero V, Vera P (1997) Two *PR-1* genes from tomato are differentially regulated and reveal
1305   a novel mode of expression for a pathogenesis-related gene during the hypersensitive response and development. Mol.
1306   Plant Microbe Interact. 10: 624-634.
1307   Trouvelot A, Kough JL, Gianinazzi-Pearson V (1986) Mesure du taux de mycorhization VA d'un system radiculaire.
1308   Recherche de methods d'estimation ayant une signification fonctionnele, in *Mycorrhizae: Physiology and Genetics*
1309   (Gianinazzi-Pearson V and Gianinazzi S eds), INRA, Paris. pp 217-222.
1310

van der Heijden MG, Martin FM, Selosse MA, Sanders IR (2015). Mycorrhizal ecology and evolution: the past, the present, and the future. New Phytol. 205: 1406-1423.

van Verk MC, Pappaioannou D, Neeleman L, Bol JF, Linthorst HJ (2008) A novel WRKY transcription factor is required for induction of PR-1a gene expression by salicylic acid and bacterial elicitors. Plant Physiol. 146: 1983-1995.

Volpe V, Giovannetti M, Sun XG, Fiorilli V, Bonfante P (2016) The phosphate transporters LjPT4 and MtPT4 mediate early root responses to phosphate status in non mycorrhizal roots. Plant Cell Environ. 39: 660-671.

Volpe V, Chitarra W, Cascone P, Volpe MG, Bartolini P, Moneti G, Pieraccini G, Di Serio C, Maserti B, Guerrieri E and Balestrini R (2018) The association with two different arbuscular mycorrhizal fungi differently affects water stress tolerance in tomato. Front. Plant Sci. 9: 1480.

von Sivers L, Jaspar H, Johst B, Roese M, Bitterlich M, Franken P, Kühn C (2019) Brassinosteroids affect the symbiosis between the AM fungus *Rhizoglomus irregularis* and solanaceous host plants. *Front. Plant Sci.* 10: 571.

Walter MH, Floss DS, Strack D (2010) Apocarotenoids: hormones, mycorrhizal metabolites and aroma volatiles. Planta 232: 1-17.

Wang KL-C, Li H, Ecker JR (2002) Ethylene biosynthesis and signaling networks. Plant Cell S131-S151.

Wang W., Shi J., Xie Q., Jiang Y., Yu N., Wang E. (2017). Nutrient exchange and regulation in arbuscular mycorrhizal symbiosis. Mol. Plant. 10: 1147-1158.

Wang M, Wilde J, Baldwin IT, Groten K (2018a) *Nicotiana attenuata*'s capacity to interact with arbuscular mycorrhiza alters its competitive ability and elicits major changes in the leaf transcriptome. J. Integr. Plant Biol. 60: 242-261.

Wang Y Zou W, Xiao Y, Cheng L, Liu Y, Gao S Shi Z, Jiang Y, Qi M, Xu T, Li T (2018b) *MicroRNA1917* targets *CTR4* splice variants to regulate ethylene responses in tomato. J. Exp. Bot. 69: 1011-1025.

Wasternack C, Hause B (2013) Jasmonates: biosynthesis, perception, signal transduction and action in plant stress response, growth and development. An update to the 2007 review in Annals of Botany. Ann. Bot. 111: 1021-1058.

Wei Z, Li J (2016) Brassinosteroids regulate root growth, development, and symbiosis. Mol. Plant 9: 86-100.

Whiteside MD, Garcia MO, Treseder KK (2012) Amino acid uptake in arbuscular mycorrhizal plants. PLoS ONE 7: e47643.

Winkler R (2015) SpiderMass: Semantic database creation and tripartite metabolite identification strategy. J. Mass Spectrom. 50: 538-541.

Xu GH, Chague V, Melamed-Bessudo C, Kapulnik Y, Jain A, Raghothama KG, Levy AA, Silber A (2007) Functional characterization of LePT4: a phosphate transporter in tomato with mycorrhiza-enhanced expression. J. Exp. Bot. 58: 2491-2501.

Yu N, Luo D, Zhang X, Liu J, Wang W, Jin Y, Dong W, Liu J, Liu H, Yang W, Zeng L, Li Q, He Z, Oldroyd GE, Wang E (2014) A DELLA protein complex controls the arbuscular mycorrhizal symbiosis in plants. Cell Res. 24: 130-133.

Zare-Maivan H, Khanpour-Ardestani N, Ghanati F (2017) Influence of mycorrhizal fungi on growth, chlorophyll content, and potassium and magnesium uptake in maize, J. Plant Nutr. 40: 2026-2032.

Zhang J, Liu H, Sun J, Li B, Zhu Q, Chen S, Zhang H (2012). Arabidopsis fatty acid desaturase FAD2 is required for salt tolerance during seed germination and early seedling growth. PLOS ONE 7: e30355.

1366
1367 Zhang Y, Hu L, Yu D, Xu K, Zhang J, Li X, Wang P, Chen G, Liu Z, Peng C, Li C, Guo T (2019) Integrative analysis
1368 of the wheat *PHT1* gene family reveals a novel member involved in arbuscular mycorrhizal phosphate transport and
1369 immunity. Cells 8: 490.

1370

1371

1372

1373

1374

1375
1376
1377
1378

Figure 1

Degree of arbuscular mycorrhizal fungi (AMF) colonization at (a) 32 days post inoculation (dpi) and (b) 45 dpi, in roots of wild type (WT) and *spr2* tomato plants inoculated with a consortium of six AMF species.

Box-and-whisker plots show high, low, and median percentage values of hyphae (H), vesicles (V) and arbuscules (A) quantified in in the root system of wild type (WT) and *spr2* mutant tomato plants. Asteriscks over the box-and-whisker plots represent statistically significant differences at $p \leq 0.05$ (*), 0.01 (**) or 0.001 (***) (Tukey Kramer test; n = 10).

(a)

(b)
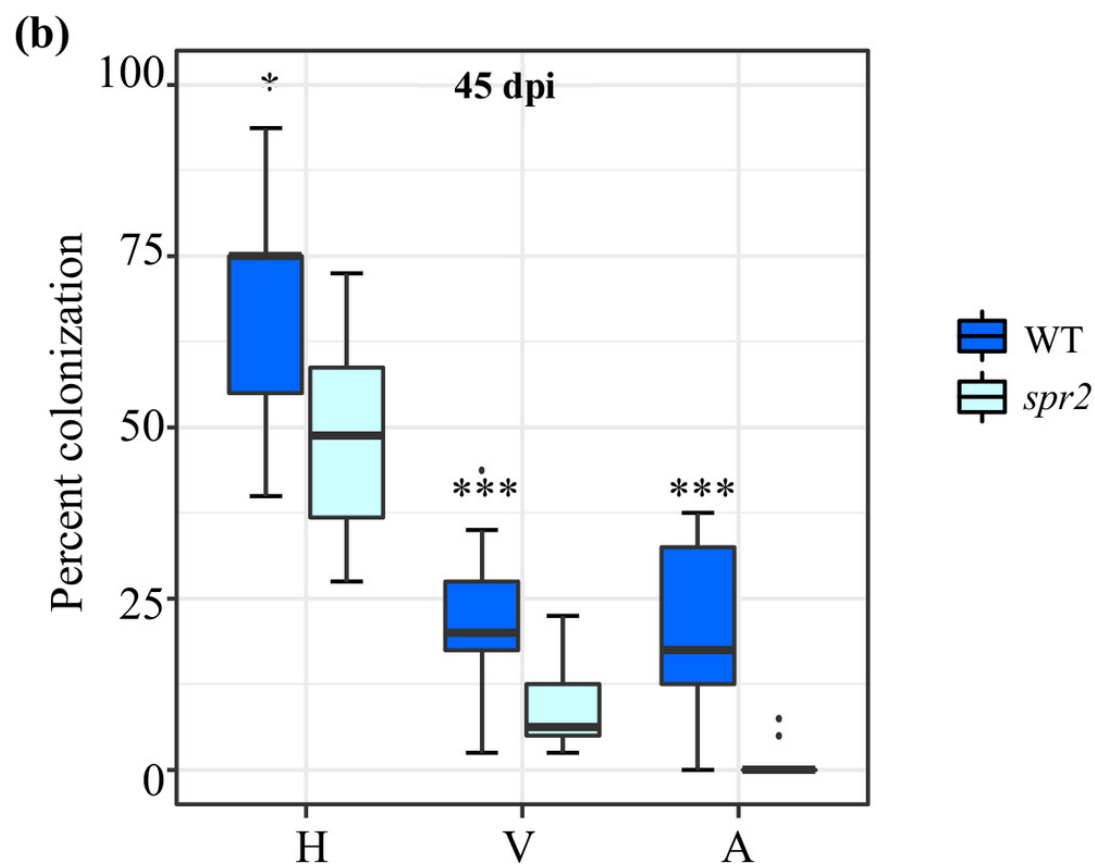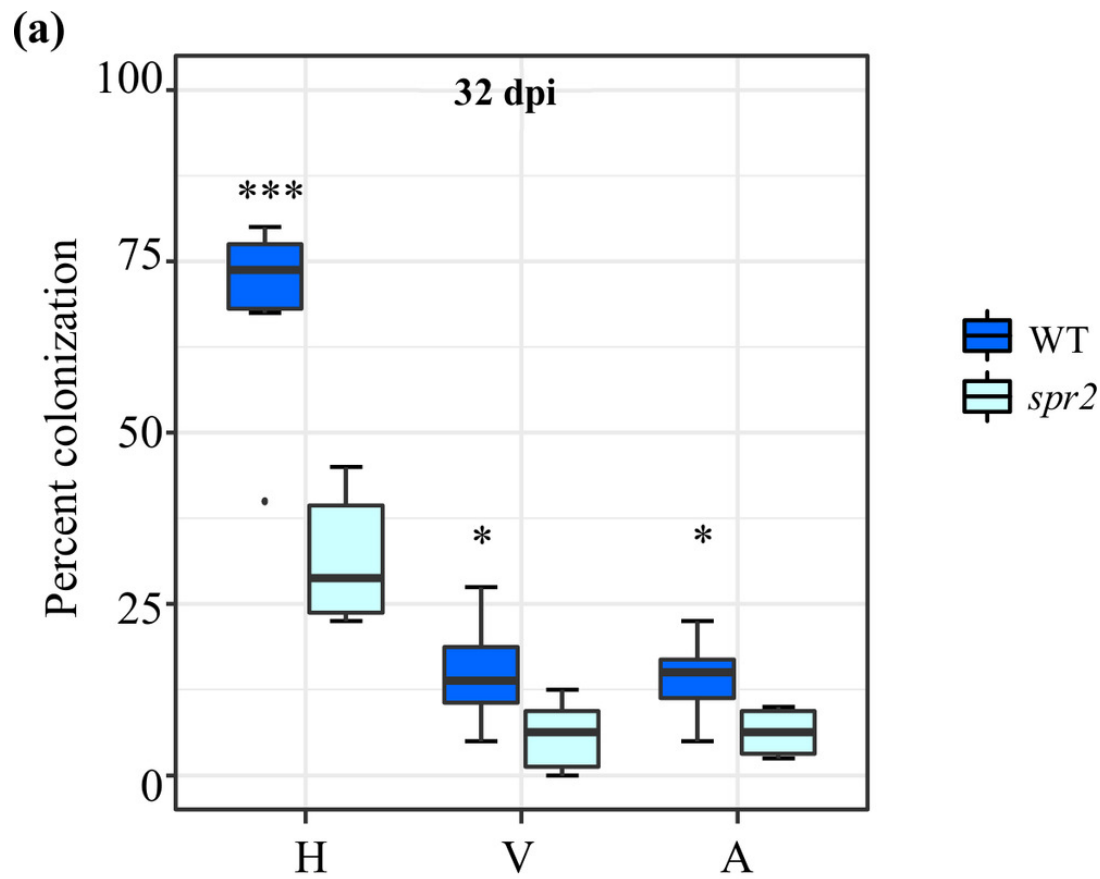
Figure 2

Modification of jasmonic acid (JA) and salicylic acid (SA) levels in response to mycorrhizal colonization.

Content of (**a**) and (**b**) JA, and (**c**) and (**d**) SA were determined in leaves (JA-L, SA-L) and roots (JA-R, SA-R) of control wild-type (WT) and *spr2* mutant tomato plants or of mycorrhizal WT (WT-M) and *spr2* (*spr2*-M) plants sampled 45 dpi. Box-and-whisker plots show high, low, and median values. Different letters over the box-and-whisker plots represent statistically significant differences at $p \leq 0.05$ (Tukey Kramer test; n = 10).
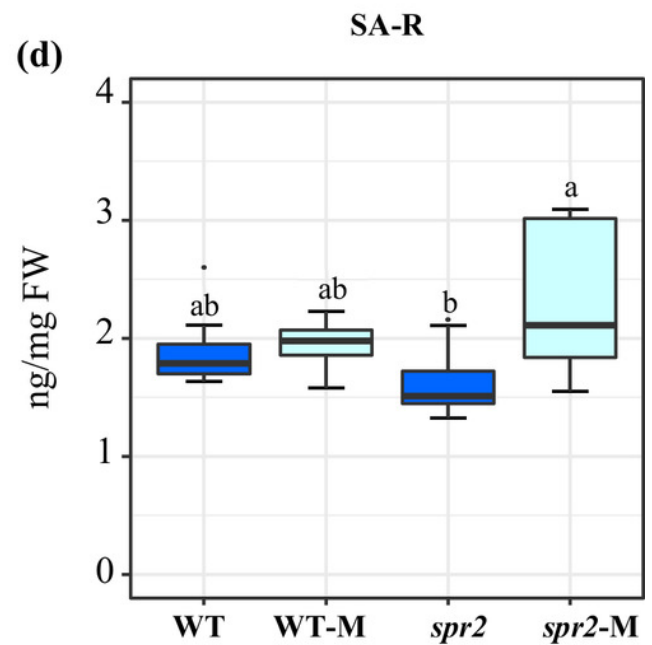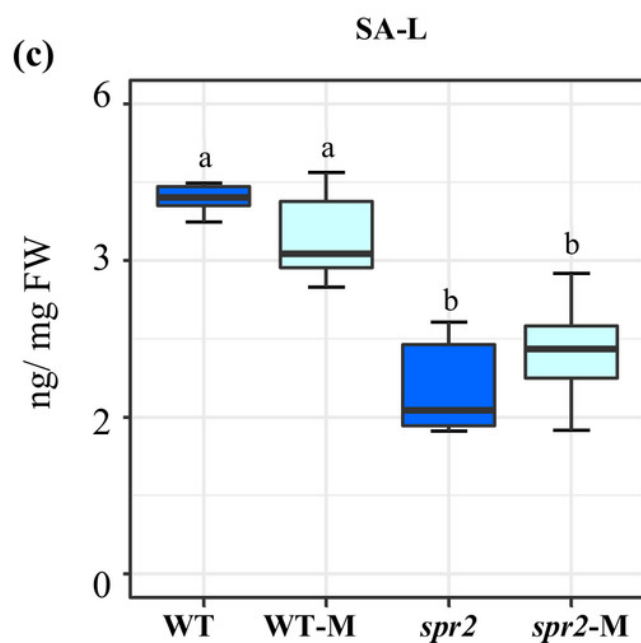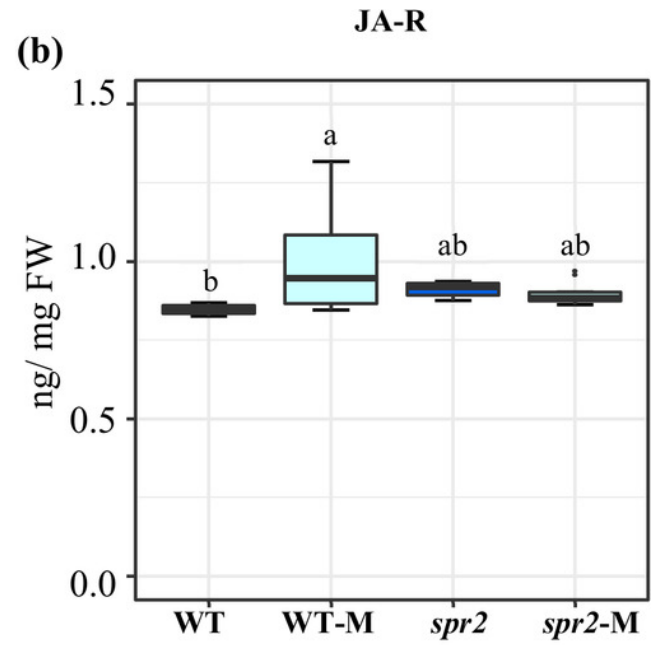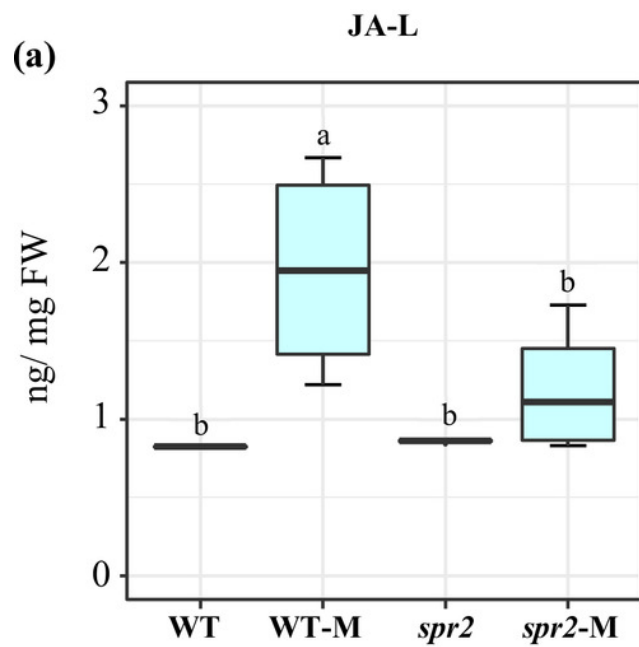
Figure 3

Untargeted principal components analysis on metabolic fingerprinting of non-colonized and mycorrhizal wild-type (WT) and *spr2* mutant tomato roots.

The intensity of 367 metabolites sampled from WT and *spr2* roots at **(a)** and **(b)** 32 dpi, and **(c)** and **(d)** 45 dpi, was used to construct a matrix to evaluate the global variance at the metabolic level in WT and mutant *spr2* genotypes in response to AMF colonization (WT-M and *spr2*-M, respectively). The three principal components explain 39.2 % and 48.8% of the total variance at 32 and 45 dpi, respectively. They were sufficient to separate the data by plant genotype and treatment. Prediction ellipses are such that they predict with 95% probability that any new observation from the same group will fall inside the ellipse. n = 12.
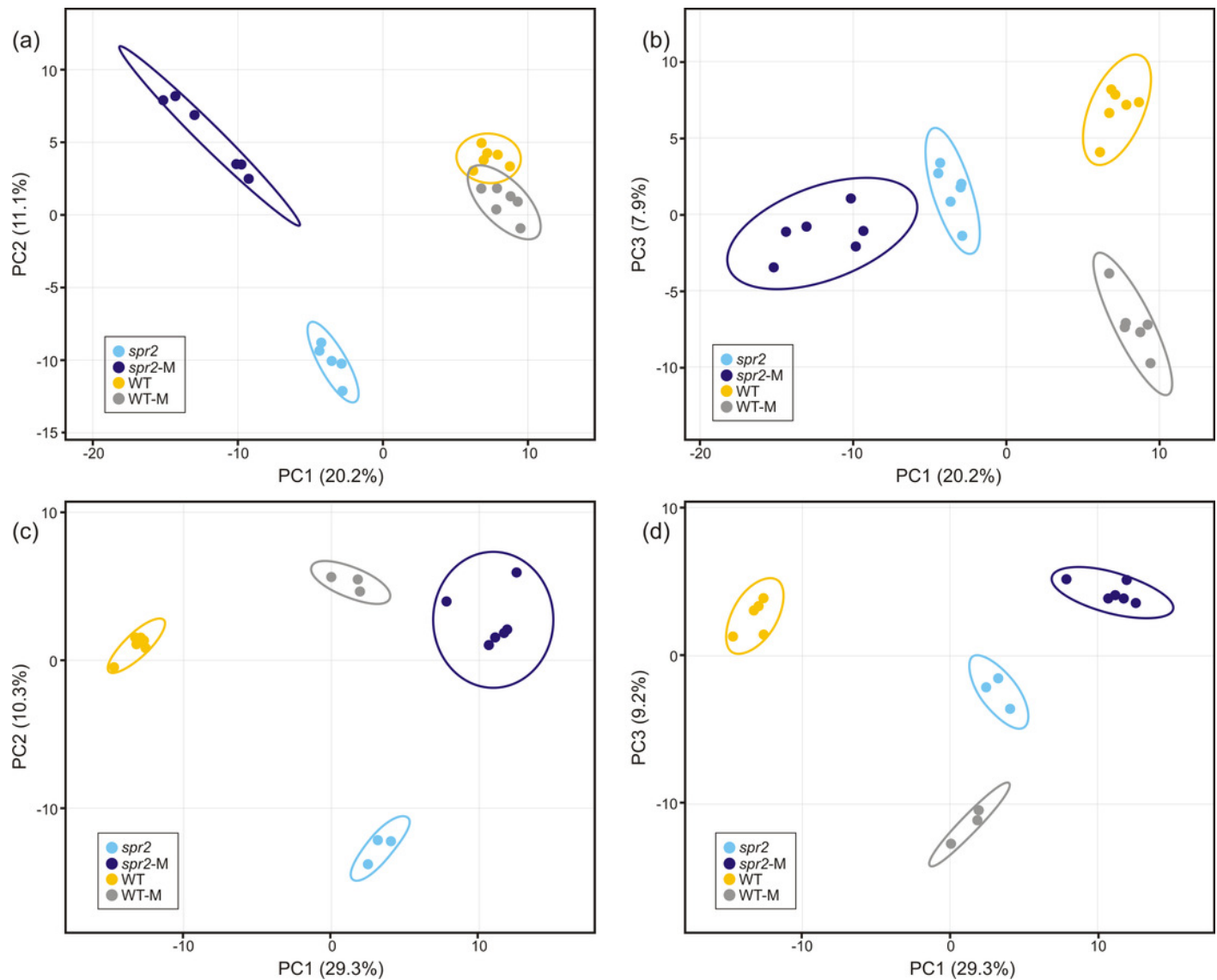
Figure 4

Metabolic heat-map generated with the 100 most intense ions detected in roots of control wild-type (WT) and *spr2* mutant tomato plants or in roots of mycorrhizal WT (WT-M) and *spr2* (*spr2*-M) plants sampled at 32 and 45 dpi.

Ions in aqueous methanol root extracts were detected by DLI-ESI-MS as described in Materials and Methods. The hierarchical clustering analysis resulted in a correct assignment of plants into well-defined clusters denoting genotype (WT *vs. spr2*), treatment (control *vs.* M) and treatment duration (32 *vs.* 45 dpi). The *m/ z* values were extracted for putative assignation (refer to Tables S2 and S3).
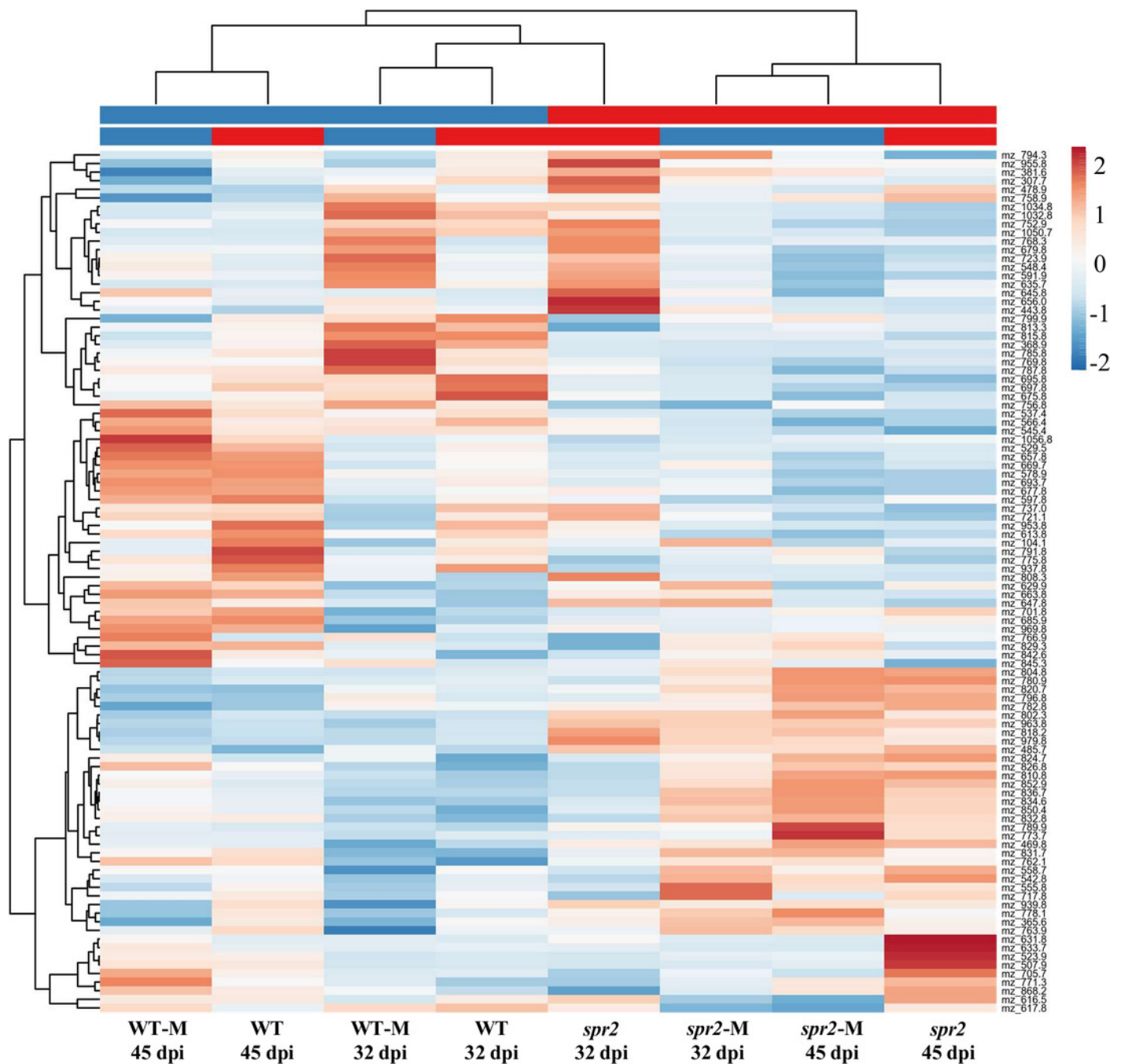
Figure 5

Modification of tomatine and total steroid glycoalkaloid contents in response to mycorrhizal colonization.

Content of (**a**) and (**b**) tomatine, and (**c**) and (**d**) total steroid glycoalkaloid ions (SGA$_T$) determined in roots of control wild-type (WT) and *spr2* mutant tomato plants or of mycorrhizal WT (WT-M) and *spr2* (*spr2*-M) plants sampled at 32 and 45 dpi, respectively. Box-and-whisker plots show high, low, and median values. Different letters over the box-and-whisker plots represent statistically significant differences at $p \leq 0.05$ (Tukey Kramer test; n = 10).

(a)

(b)

(c)

(d)
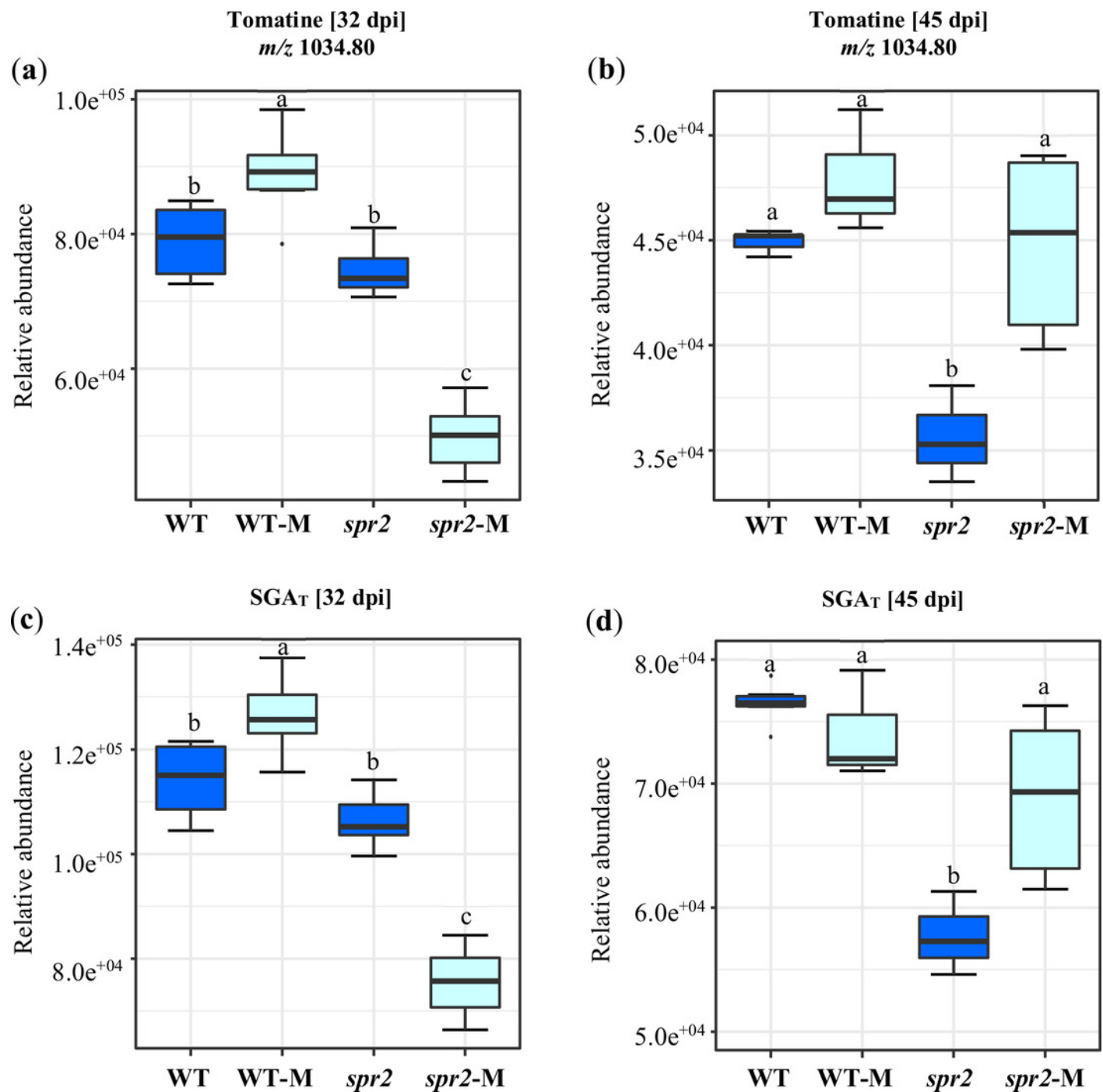
Gene expression levels in roots of mycorrhizal wild-type (WT) and *spr2* mutant tomato plants.

The expression levels[1] shown were obtained from non-mycorrhizal roots and mycorrhizal roots colonized for 32, 45 and 50 dpi.

Colonization period	32 dpi						45 dpi						50 dpi					
Genotype/ Treatment	WT [C][2]	WT [M][3]	WT [M/C][4]	spr2 [C]	spr2 [M]	spr2 [M/C]	WT [C]	WT [M]	WT [M/C]	spr2 [C]	spr2 [M]	spr2 [M/C]	WT [C]	WT [M]	WT [M/C]	spr2 [C]	spr2 [M]	spr2 [M/C]
Gene/ Gene category	Mycorrhizal colonization marker																	
LePT4	0.008	4.46	560[6]	0.003	4.76	1746	0.02	2.52	140	0.004	1.73	403	0.001	1.97	2377	0.003	0.50	185
	Brassinosteroids																	
DET 2	0.55	0.24	0.44[7]	0.27	0.66	2.45	0.70	0.29	0.42	0.28	0.30	1.09	1.15	2.16	1.88	0.81	0.69	0.85
DWF4	0.27	0.14	0.53	0.07	0.27	3.77	0.10	0.02	0.22	0.05	0.10	2.03	0.31	0.10	0.32	0.24	0.25	1.04
CPD	0.34	0.15	0.45	0.16	0.32	2.01	0.15	0.08	0.55	0.12	0.03	0.23	0.16	0.17	1.08	0.10	0.17	1.79
	Gibberellins																	
CPS	0.003	0.05	14.30	0.004	0.03	8.30	0.02	0.07	4.17	0.012	0.006	0.48	0.01	0.10	7.80	0.009	0.011	1.21
KS	0.47	0.17	0.37	0.30	0.33	1.07	0.27	0.24	0.90	0.36	0.28	0.78	0.69	0.39	0.56	0.43	0.52	1.23
GA3ox	0.01	0.33	23.6	0.02	1.09	69.0	0.03	0.39	14.1	0.03	0.45	15.4	0.02	0.68	29.9	0.01	0.26	32.7
GAI	1.63	0.53	0.33	1.14	6.17	5.39	0.65	0.37	0.57	2.91	2.18	0.75	48.6	13.9	0.29	14.9	25.5	1.71
	Abscisic acid																	
TAS14	-[5]	-	-	-	-	-	-	-	-	-	-	-	248	375	1.51	444	746	1.68
NCED1	-	-	-	-	-	-	-	-	-	-	-	-	0.99	1.96	1.99	1.29	1.92	1.49
	Apocarotenoids																	
CCD7	0.01	0.12	10.9	0.01	0.24	33.6	0.04	0.27	6.81	0.03	0.42	16.7	0.14	0.79	5.51	0.09	0.19	2.10
CCD1a	-	-	-	-	-	-	-	-	-	-	-	-	1.34	0.94	0.70	0.94	0.98	1.04
CCD1b	1.44	0.85	0.59	1.04	2.15	2.06	1.13	0.60	0.53	0.74	1.25	1.68	2.63	1.02	0.39	3.47	3.35	0.97
	9-LOX																	
HPL	-	-	-	-	-	-	-	-	-	-	-	-	2.19	5.98	2.73	1.66	3.64	2.19
LOXA	-	-	-	-	-	-	-	-	-	-	-	-	3.67	3.81	1.04	0.75	1.08	1.44
DES	-	-	-	-	-	-	-	-	-	-	-	-	3.05	9.47	3.10	3.34	5.73	1.72
AOS 3	-	-	-	-	-	-	-	-	-	-	-	-	1.12	7.18	6.43	0.03	0.17	5.19
	13-LOX																	
LOXD	3.08	4.39	1.43	1.65	2.33	1.41	0.26	0.30	1.16	0.28	0.42	1.47	14.8	7.60	0.51	14.4	10.4	0.72
AOS 1	-	-	-	-	-	-	-	-	-	-	-	-	4.49	3.68	0.82	2.85	2.81	0.98
JAZ 2	1.78	9.99	5.62	3.81	5.72	1.50	0.44	0.33	0.75	0.16	0.28	1.71	10.2	17.3	1.70	12.9	4.46	0.34
JMT	0.98	1.53	1.56	0.63	2.16	3.44	0.27	0.76	2.85	0.23	1.12	4.87	0.59	1.81	3.09	0.86	0.62	0.72

Wound response																		
PS	0.0009	0.0012	1.33	0.001	0.003	**3.68**	0.0017	0.0016	0.93	0.0013	0.0010	0.79	0.0023	0.0047	**2.01**	0.0028	0.0011	**0.39**
RBOH1	0.30	0.07	**0.24**	0.09	0.23	**2.63**	0.33	0.14	**0.42**	0.22	0.16	0.73	0.26	0.13	**0.51**	0.23	0.13	**0.55**
LHA1	3.11	1.11	**0.36**	1.51	2.24	**1.48**	1.35	1.19	0.88	1.25	0.82	0.65	2.40	2.35	0.98	1.88	2.74	**1.46**
PLA2	-	-	-	-	-	-	-	-	-	-	-	-	0.57	0.49	0.85	0.54	0.63	1.18
PINII	0.41	0.74	**1.79**	0.45	3.13	**6.95**	0.013	0.005	**0.40**	0.0025	0.0015	**0.62**	0.68	0.20	**0.30**	0.11	0.05	**0.41**
AroGP3	0.21	0.04	**0.22**	0.08	0.12	**1.51**	0.61	0.30	**0.49**	0.72	0.45	**0.63**	1.27	0.27	**0.21**	0.53	0.49	0.92
PPO	-	-	-	-	-	-	-	-	-	-	-	-	4.87	9.58	**1.97**	0.82	1.73	**2.11**
CYP2	25.8	19.3	0.75	14.5	20.6	**1.42**	39.2	30.6	0.78	51.4	43.2	0.84	72.4	122	**1.69**	19.2	52.0	**2.70**
SCP	0.21	0.07	**0.35**	0.23	0.30	1.28	0.72	0.35	**0.49**	0.69	0.38	**0.55**	0.35	0.25	0.72	0.18	0.33	**1.81**
Ethylene Biosynthesis																		
ACS2	0.03	0.01	**0.47**	0.05	0.15	**2.87**	0.03	0.01	**0.40**	0.02	0.03	**1.46**	0.47	0.11	**0.23**	0.24	0.11	**0.44**
ACS6	-	-	-	-	-	-	-	-	-	-	-	-	25.5	16.8	**0.66**	7.26	11.7	**1.61**
ACO4	3.13	2.22	0.71	3.24	5.70	**1.76**	2.53	3.20	1.27	3.54	1.77	**0.50**	47.3	40.2	0.85	12.6	25.8	**2.04**
Ethylene Signaling																		
CTR4	-	-	-	-	-	-	-	-	-	-	-	-	2.21	3.35	**1.52**	1.94	1.64	0.85
EIN2	1.00	0.30	**0.30**	0.23	0.34	**1.49**	1.12	0.73	0.65	1.07	0.12	**0.11**	8.32	6.49	0.78	4.70	14.07	**2.99**
EIN3	0.27	0.17	0.64	0.20	0.58	**2.86**	0.25	0.25	0.99	0.21	0.09	**0.45**	1.45	1.29	0.89	1.50	5.80	**3.86**
ERF1b	-	-	-	-	-	-	-	-	-	-	-	-	0.20	2.40	**12.03**	0.09	0.97	**11.15**
Salicylic acid signaling																		
PR1	0.105	0.011	**0.10**	0.03	0.05	**2.01**	0.11	0.04	**0.31**	0.07	0.08	1.23	-	-	-	-	-	-
SSI2	0.008	0.007	0.94	0.003	0.015	**5.05**	0.0014	0.0013	0.88	0.0023	0.0004	**0.15**	-	-	-	-	-	-
SAMT	0.006	0.002	**0.34**	0.01	0.04	**3.81**	0.14	0.10	0.68	0.31	0.42	1.35	-	-	-	-	-	-
WRKY60	0.81	0.69	0.85	0.37	0.65	**1.78**	0.84	0.82	0.98	1.12	0.42	**0.38**	-	-	-	-	-	-
Phenylpropanoid/ phenolic compounds biosynthesis																		
PAL3	6.09	2.17	**0.36**	2.84	9.20	**3.24**	3.93	2.28	**0.58**	3.86	3.88	1.01	55.9	27.4	**0.49**	31.2	22.4	0.72
PAL 4	61.3	72.6	1.18	32	88	**2.74**	66.1	42.4	0.64	33.4	30.4	0.91	795	341	**0.43**	407	367	0.90
PAL 5	-	-	-	-	-	-	-	-	-	-	-	-	39.1	54.6	**1.40**	50.1	54.5	1.09
FLS	-	-	-	-	-	-	-	-	-	-	-	-	0.52	1.27	**2.46**	0.46	1.04	**2.26**
Isoprenoid biosynthesis/ volatiles																		
DXS-2	-	-	-	-	-	-	-	-	-	-	-	-	0.14	0.78	**5.51**	0.09	0.12	1.37
FPS1	1.59	1.22	0.77	0.86	2.72	**3.15**	4.47	2.43	**0.54**	3.19	3.69	1.16	4.62	2.21	**0.48**	1.81	1.47	0.81
HMGR 1	-	-	-	-	-	-	-	-	-	-	-	-	4.56	2.94	0.64	4.34	4.53	1.04
BEAT	-	-	-	-	-	-	-	-	-	-	-	-	0.30	2.92	**9.87**	0.06	0.07	1.16
Glycoalkaloid biosynthesis																		
GAME 1	0.32	0.15	**0.49**	0.23	0.46	**1.97**	2.01	1.19	**0.59**	1.16	0.83	0.72	1.19	0.88	0.74	0.68	0.91	1.35

CAS 1	0.40	0.16	**0.40**	0.23	0.57	**2.55**	0.56	0.28	**0.50**	0.33	0.34	1.05	0.42	0.48	1.14	0.34	0.49	**1.41**

2   [1]Gene expression levels were calculated using the $2^{-\Delta Ct}$ equation, according to Livak and Schmittgen (2001).
3   [2]**C**, represents expression levels quantified in roots of non-mycorrhizal control plants.
4   [3]**M**, represents expression levels quantified in roots of mycorrhizal plants.
5   [4]**M/C**, represents the gene expression ratio between roots of mycorrhizal and non-mycorrhizal plants.
6   [5]The **(-)** symbol indicates that gene expression at these time points was not determined.
7   [6]M/C values in **bold text** indicate a positive influence on gene expression by AMF colonization.
8   [7]M/C values in **red bold text** indicate a negative influence on gene expression by AMF colonization.
9
10

Effect of mycorrhizal colonization on metabolite abundance in roots of wild-type (WT) and *spr2* mutant tomato plants.

Metabolite quantitation was determined in roots of control and mycorrhizal plants of both

genotypes, sampled after a 45 dpi mycorrhizal colonization period[1].

Metabolites	Genotype/ treatment ratios[2]			
	WT/ *spr2*	WT-M/ WT	*spr2*-M/ *spr2*	WT-M/ *spr2*-M
1, 3-Pentadiene	**0.81[4]**	**2.10[3]**	1.09	1.56
Glyoxylic oxime acid	0.76	1.61	0.72	1.72
Phosphoric acid	**0.76**	**2.35**	**2.27**	0.78
n-Butylamine	1.07	1.36	0.73	2.00
Diethylene glycol	0.85	**2.29**	**1.34**	1.46
4, 6-Dimethyl dodecane,	1.11	2.13	**1.72**	1.38
Glycerol	**0.42**	**2.17**	0.91	1.01
Maleic acid	**0.66**	1.30	**0.82**	1.05
Succinic acid	**0.76**	**1.48**	**1.11**	1.01
Propanoic acid	**0.83**	**1.47**	**1.34**	0.91
Fumaric acid	**0.76**	**1.68**	**1.30**	0.98
Furanone	0.90	**2.11**	**1.69**	1.13
DL-malic acid	**0.81**	0.95	1.09	**0.71**
L-proline	**0.51**	**1.63**	**0.69**	1.21
m-Hydroxybenzoic acid	1.04	1.60	**2.30**	0.72
L-threonic acid	**0.56**	**1.32**	**1.16**	**0.64**
1-Cyclohexene-3, 4,5-trihydroxy-1-carboxylic acid	**1.46**	1.04	**1.70**	0.90
Isocitric acid	1.02	**0.86**	**0.91**	0.97
D-fructose	**1.29**	0.80	0.74	1.40
D-glucose	**1.07**	**0.75**	0.67	1.21
Myo-inositol	0.98	0.82	1.01	0.79
D-glucuronic acid,	1.14	1.55	1.50	1.17
Sucrose	**1.18**	0.75	0.87	1.02

2 [1]The targeted metabolite analysis was performed by GC-MS.
3 [2]The ratios were determined using the mean peak areas of each compound.
4 [3]Numbers in bold in a green background indicate a significantly higher ratio.
5 [4]Numbers in bold in a red background indicate a significantly lower ratio.

Effect of mycorrhizal colonization on metabolite abundance in leaves of wild-type (WT) and *spr2* mutant tomato plants.

Metabolite quantitation was determined in leaves of control and mycorrhizal plants of both

genotypes, sampled after a 45 dpi mycorrhizal colonization period[1].

METABOLITES	Genotype/ treatment ratios[2]			
	WT/ *spr2*	WT-M/ WT	*spr2*-M/ *spr2*	WT-M/ *spr2*-M
1, 3-Pentadiene	1.34	0.80	0.92	1.17
Glyoxylic oxime acid	1.09	1.10	0.88	1.36
Propanoic acid	1.25	0.87	0.88	1.24
Phosphoric acid	**1.53**[3]	1.38	**0.72**	**2.92**
2-Butenoic acid	**5.36**	0.72	1.29	**3.00**
Benzoic acid	1.50	0.93	0.75	**1.87**
Diethylene glycol	1.13	1.01	**0.78**	**1.48**
Serine	**0.22**[4]	**3.64**	**0.49**	1.63
4, 6-dimethyl dodecane	1.06	1.26	0.69	**1.92**
Glycerol	**0.77**	0.99	1.11	**0.69**
Maleic acid	**0.53**	1.09	**1.33**	**0.43**
Succinic acid	**1.15**	1.05	1.26	0.96
Butanedioic acid, methyl	**1.19**	1.00	**0.68**	**1.76**
Propanoic acid	1.10	1.09	0.83	**1.44**
Fumaric acid	**0.85**	1.07	0.93	0.98
Furanone	0.77	**1.39**	0.87	1.24
L-aspartic acid	1.37	**0.55**	1.27	0.59
D-(-)-citramalic acid	1.11	1.16	1.16	1.10
DL-malic acid	0.90	1.38	0.94	**1.32**
L-proline, 5-oxo	**0.47**	**1.63**	1.71	**0.45**
m-Hydroxybenzoic acid	1.02	1.05	**0.68**	**1.57**
L-threonic acid	**1.72**	0.78	1.09	1.23
Phenylpyruvic acid	**1.68**	0.77	**0.82**	**1.57**
1-Cyclohexene-3, 4, 5-trihydroxy-1-carboxylic acid	**2.19**	**0.61**	0.90	**1.48**
Isocitric acid	1.07	0.89	1.00	0.96
D-fructose	**0.62**	**1.44**	**1.20**	**0.74**
D-glucose	**0.54**	**1.40**	1.03	**0.74**
Myo-inositol	1.11	**0.84**	0.92	1.01
Phytol	1.26	0.84	0.91	1.18
D-glucuronic acid	**2.46**	**0.62**	**1.19**	**1.28**
Sucrose	**1.22**	**0.87**	**0.80**	**1.33**

2   [1]The targeted metabolite analysis was performed by GC-MS.

3   [2]The ratios were determined using the mean peak areas of each compound.

4   [3]Numbers in bold in a green background indicate a significantly higher ratio.

5   [4]Numbers in bold in a red background indicate a significantly lower ratio.

Effect of mycorrhizal colonization on fatty acid abundance in roots of wild-type (WT) and *spr2* mutant tomato plants.

Fatty acids were quantified in roots of control and mycorrhizal plants of both genotypes,

sampled after a 45 dpi mycorrhizal colonization period[1].

FATTY ACID	% abundance[2]			Genotype/ treatment ratios			
	WT	*spr2*		WT/ *spr2*	WT-M/ WT	*spr2*-M/ *spr2*	WT-M/ *spr2*-M
C14:0 (myristic acid)	0.40	0.28		**1.42**[3]	0.98	1.00	**1.39**
C14:0 (13-methyl)	0.69	0.53		**1.32**	0.92	0.98	**1.23**
C15:0	0.62	0.48		**1.28**	0.99	1.02	**1.25**
C15:0 (14-methyl)	0.48	0.37		**1.31**	1.04	1.00	**1.36**
C16:0 (palmitic acid)	21.22	21.70		0.98	**1.23**	0.97	**1.23**
C16:0 (15-methyl)	2.92	2.39		**1.22**	**0.93**	1.03	**1.10**
C16:1 (9Z) (palmitoleic acid)	1.13	0.69		**1.64**	0.85	1.12	1.26
C18:0 (stearic acid)	3.24	2.38		**1.36**	0.93	1.09	**1.17**
C18:1 (9Z) (oleic acid)	2.33	1.33		1.75	1.17	**1.09**	1.86
C18:1 (9E) (elaidic acid)	0.86	1.26		**0.69**[4]	**2.38**	0.76	**2.14**
C18:2 (linoleic acid)	41.55	52.44		**0.79**	0.99	1.00	**0.78**
C18:3 (linolenic acid)	6.60	3.14		**2.10**	0.90	1.00	**1.90**
C20:0 (eicosanoic acid)	2.04	1.51		**1.35**	**0.71**	1.07	0.90
C22:0 (behenic acid)	10.69	7.94		**1.35**	**0.70**	1.01	0.94
C24:0 (lignocceric acid)	5.23	3.56		**1.47**	**0.83**	1.02	**1.20**

2   [1]FA analysis was performed by GC-MS.
3   [2]% Abundance determined using the mean peak areas of each FA.
4   [3]Numbers in bold in a green background indicate a significantly higher ratio.
5   [4]Numbers in bold in a red background indicate a significantly lower ratio.

Effect of mycorrhizal colonization on fatty acid abundance in leaves of wild-type (WT) and *spr2* mutant tomato plants.

Fatty acids were quantified in leaves of control and mycorrhizal plants of both genotypes,

sampled after a 45 dpi mycorrhizal colonization period[1].

FATTY ACIDS	% abundance[2]		Genotype/ treatment ratios			
	WT	*spr2*	WT/ *spr2*	WT-M/ WT	*spr2*-M/ *spr2*	WT-M/ *spr2*-M
C14:0 (myristic acid)	0.08	0.06	1.39[5]	1.00	1.07	1.31
C15:0	0.04	0.05	0.90	1.05	0.99	0.96
C16:0 (palmitic acid)	16.95	15.82	1.07	1.18	1.01	1.25
C16:0 (14 Me)	0.25	0.22	1.14	1.16	0.65	2.02
C16:1 (7E) (palmitelaidic acid)	1.06	1.46	0.72	1.30	0.77	1.23
C16:1 (9Z) (palmitoleic acid)	0.29	0.32	0.90	1.03	0.90	1.03
C16:2 (palmitlinoleic acid)	0.40	4.84	0.08[6]	1.02	1.06	0.08
C16:3	6.58	--[3]	--[4]	0.85	--	--
C18:0 (stearic acid)	1.45	1.12	1.29	1.14	1.32	1.11
C18:1 (9E)	0.44	0.39	1.13	1.10	0.94	1.31
C18:2 (linoleic acid)	12.54	71.71	0.17	1.42	1.01	0.25
C18:3 (linolenic acid)	58.84	3.10	18.99	0.86	0.76	21.45
C18:4 (parinaric acid)	0.11	--	--	2.34	--	--
C20:0 (eicosanoic acid)	0.36	0.32	1.11	1.14	0.81	1.57
C22:0 (behenic acid)	0.27	0.31	0.89	1.12	1.03	0.97
C24:0 (lignoceric acid)	0.34	0.28	1.21	1.12	0.91	1.48

2   [1]FA analysis was performed by GC-MS.
3   [2]% Abundance determined using the mean peak areas of each FA.
4   [3]Fatty acid not detected.
5   [4]Ratio could not be determined.
6   [5]Numbers in bold in a green background indicate a significantly higher ratio.
7   [6]Numbers in bold in a red background indicate a significantly lower ratio.

Changes in the abundance of α-tomatine and related compounds in roots at 32 dpi.

The content of α-tomatine, its biosynthetic precursors and catabolic products were determined in roots of wild-type (WT) and *spr2* mutant tomato plants after a 32 dpi mycorrhizal colonization period[1].

Ion identity	Putative metabolite[1]	Wt/ *spr2*	Wt-M/ Wt	*spr2*-M/ *spr2*	Wt-M/ *spr2*-M
mz_413.94	Dehydrotomatine (tomatidenol)	0.74	0.97	0.90	0.79
mz_416.89	Tomatidine and isomers	0.91	0.97	1.09	0.81
mz_576.89	ND[2]	0.95	1.13	0.98	1.10
mz_578.93	ND	1.08	1.02	0.96	1.15
mz_916.75	Hydroxydehydrotomatidine Trihexoside and isomers	0.79	1.19	0.76	1.23
mz_1004.64	Tomatidine dihexoside dipentoside and isomers	0.97	1.16	0.71	1.58
mz_1018.01	Tomatidine + dihexoside + pentose + deoxyhexose	1.63	0.74	1.02	1.18
mz_1030.6	Di-dehydrotomatine	0.83	1.44	0.76	1.56
mz_1032.75	Dehydrotomatine and isomers	1.28[5]	1.12	0.78	1.82
mz_1034.8	α-Tomatine and isomers	1.06	1.13	0.67	1.78
mz_1044.78	UGA 4[3]	0.77	1.20	0.84	1.10
mz_1046.84	UGA 5	0.80[6]	1.28	0.71	1.45
mz_1050.7	Hydroxytomatine and isomers	0.93	1.04	0.54	1.79
mz_1056.78	ND	1.22	0.92	1.09	1.03
mz_1064.77	Tomatidine tetrahexoside	1.18	1.16	0.80	1.71
mz_1072.72	ND	1.31	1.02	1.02	1.31
mz_1090.77	Acetoxy-dehydrotomatine	1.06	0.96	0.80	1.26
mz_1092.67	Acetoxytomatine	1.09	0.88	0.60	1.59
	Total SGAs[4]	1.07	1.11	0.71	1.67

1 [1]Putative metabolite according to Itkin et al. (2011) Plant Cell 23: 4507-4525.
2 [2]Origin of ion not determined ion.
3 [3]Unknown glycoalkaloid
4 [4]Total steroid glycolalcaloids
5 [5]Numbers in bold in a green background indicate a significantly higher ratio.
6 [6]Numbers in bold in a red background indicate a significantly lower ratio.

Changes in the abundance of α-tomatine and related compounds in roots at 45 dpi.

The content of α-tomatine, its biosynthetic precursors and catabolic products were determined in roots of wild-type (WT) and *spr2* mutant tomato plants after a 32 dpi mycorrhizal colonization period[1].

Ion identity	Putative metabolite[1]	Wt/ spr2	Wt-M/ Wt	spr2-M/ spr2	Wt-M/ spr2-M
mz_413.94	Dehydrotomatine (tomatidenol)	1.20	0.80	0.79	1.21
mz_416.89	Tomatidine and isomers	**2.34**	**0.61**	1.04	**1.38**
mz_576.89	ND[2]	**1.69**	0.67	1.00	1.14
mz_578.93	ND	**1.74**	**0.67**	1.00	1.16
mz_916.75	Hydroxydehydrotomatidine Trihexoside and isomers	**1.61**	**0.50**	1.17	0.69
mz_1004.64	Tomatidine dihexoside dipentoside and isomers	1.46	0.99	1.21	1.20
mz_1018.01	Tomatidine + dihexoside + pentose + deoxyhexose	1.07	0.72	0.64	1.21
mz_1030.6	Di-dehydrotomatine	**1.37**	1.11	1.00	1.52
mz_1032.75	Dehydrotomatine and isomers	**1.37**	0.92	1.17	1.07
mz_1034.8	α-Tomatine and isomers	**1.26**	**1.07**	**1.26**	1.07
mz_1044.78	UGA[3] 4	1.42	0.73	1.18	0.88
mz_1046.84	UGA 5	**1.47**	**0.69**	**1.49**	**0.69**
mz_1050.7	Hydroxytomatine and isomers	**1.42**	**0.78**	**1.36**	0.81
mz_1056.78	ND	**1.27**	**1.10**	1.04	**1.35**
mz_1064.77	Tomatidine tetrahexoside	**1.49**	0.81	1.18	1.01
mz_1072.72	ND	1.24	1.06	0.83	**1.58**
mz_1090.77	Acetoxy-dehydrotomatine	1.10	0.74	1.03	0.78
mz_1092.67	Acetoxytomatine	1.11	**0.70**	1.07	**0.73**
	Total SGA[4]s	**1.32**	0.97	**1.19**	1.07

1 [1]According to Itkin et al. (2011) Plant Cell 23: 4507-4525.
2 [2]Origin of ion not determined.
3 [3]Unknown glycoalkaloid
4 [4]Total steroid glycolalcaloids
5 [5]Numbers in bold in a green background indicate a significantly higher ratio.
6 [6]Numbers in bold in a red background indicate a significantly lower ratio.